

¹ A Design for a Deep Underground Single-Phase
² Liquid Argon Time Projection Chamber for
³ Neutrino Physics and Astrophysics

⁴ March 31, 2015

Contents

| | | |
|----|---|----------|
| 2 | 1 Photon Detector | 1 |
| 3 | 1.1 Introduction | 1 |
| 4 | 1.2 Requirements and Goals | 1 |
| 5 | 1.2.1 Beam-based physics | 1 |
| 6 | 1.2.2 Proton Decay and Atmospheric Physics | 2 |
| 7 | 1.2.3 Low-energy Physics | 2 |
| 8 | 1.2.4 Required Performance | 3 |
| 9 | 1.2.5 General Considerations | 4 |
| 10 | 1.3 Photon Detector Prototype Designs | 4 |
| 11 | 1.3.1 Cast or Bulk Doped Acrylic Bars | 5 |
| 12 | 1.3.2 Fiber-embedded Bulk Acrylic Plate | 7 |
| 13 | 1.3.3 LSU Photon detection panel production | 7 |
| 14 | 1.3.4 Proof-of-Concept and Prototype Detector Results | 9 |
| 15 | 1.3.5 R&D Work in Progress and Present Plans | 11 |
| 16 | 1.3.6 Fiber Bundle with WS-coated Radiator | 12 |
| 17 | 1.4 Silicon Photomultipliers | 14 |
| 18 | 1.4.1 Requirements | 16 |
| 19 | 1.4.2 Test Results | 18 |
| 20 | 1.5 Mechanical Support | 23 |
| 21 | 1.6 Photon System Readout Electronics | 29 |
| 22 | 1.6.1 Reference Design | 29 |
| 23 | 1.6.2 Alternatives | 35 |
| 24 | 1.7 Photon Detector Calibration | 37 |
| 25 | 1.8 Installation | 43 |

List of Figures

| | | | |
|----|------|---|----|
| 2 | 1.1 | Probability of photon being detected in detectors when depositing energy | 4 |
| 3 | 1.2 | Schematic drawing of a light guide with its photosensors | 5 |
| 4 | 1.3 | LSU photon-detection panel | 8 |
| 5 | 1.4 | Light yield for the fiber LSU PD panels with alpha source in LAr | 10 |
| 6 | 1.5 | Summed charge plots of SiPMs in response to muon hodoscope trigger . | 11 |
| 7 | 1.6 | Fiber-bundle PD prototype (early one-sided version) | 13 |
| 8 | 1.7 | SiPM signals as function of bias voltage in liquid nitrogen. | 17 |
| 9 | 1.8 | The schematics of the PCB board and the PCB as built | 19 |
| 10 | 1.9 | Acrylic holder for SiPMs and assembly prior to lowering in the dewar . . | 20 |
| 11 | 1.10 | Gain test of SenSL C series SiPM in LN ₂ and numbers of p.e.'s | 21 |
| 12 | 1.11 | SiPM SenSL C series dark rate, two data runs in LN ₂ | 22 |
| 13 | 1.12 | SenSL C series SiPM afterpulsing fraction comparison, with system cooled | 22 |
| 14 | 1.13 | SenSL C series SiPM cross-talk measurement based on two runs in LN ₂ . | 23 |
| 15 | 1.14 | Full APA frame with ten photon detectors mounted inside the frame . . | 24 |
| 16 | 1.15 | Photograph of 40 cm long bar-based prototype mounted in test frame . | 26 |
| 17 | 1.16 | Mechanical assembly drawing of frame system | 27 |
| 18 | 1.17 | Blow up of APA fram showing PD insertion location | 28 |
| 19 | 1.18 | Slot and rail showing mounting location of photon detector | 28 |
| 20 | 1.19 | Block diagram of the photon detector signal processing system | 30 |
| 21 | 1.20 | Picture of the SSP module | 33 |
| 22 | 1.21 | Block diagram the SSP module | 34 |
| 23 | 1.22 | Concept of the UV-light calibration system | 40 |
| 24 | 1.23 | Diagrams of diffusers, their locations and UV light transport | 40 |
| 25 | 1.24 | Photon detector calibration module (PDCM) layout | 41 |
| 26 | 1.25 | Simulated light distributions of the 35t APA, two cases | 42 |
| 27 | 1.26 | Cable assembly for each photon detector readout channel. | 44 |
| 28 | 1.27 | Connection between the PD twisted-pair cable and SiPM mounting board. | 45 |
| 29 | 1.28 | Insertion of one PD paddle | 45 |

1

v

List of Tables

| | | | |
|---|-----|--|----|
| 2 | 1.1 | Individual photon collection efficiencies | 3 |
| 3 | 1.2 | Light guide technologies | 6 |
| 4 | 1.3 | Physics requirements for the photon detector electronics | 30 |

¹ Todo list

| | |
|---|----|
| ² In our 2012 CDR we started each chapter with: The scope of the (whichever) | |
| ³ subsystem includes the design, procurement, fabrication, testing, delivery and | |
| ⁴ installation of the mechanical and high voltage components of the (blah); | |
| ⁵ followed by list of components – see the TPC chapter. At this late date, not | |
| ⁶ sure it's worth it... | 1 |
| ⁷ when? | 2 |
| ⁸ clarify 'detector design can be found' | 2 |
| ⁹ | 3 |
| ¹⁰ (need general TPC cell map with better description) | 4 |
| ¹¹ Fuzzy at this size | 5 |
| ¹² define 'baseline' here; do you mean 'reference design'? | 7 |
| ¹³ reference? | 7 |
| ¹⁴ define | 9 |
| ¹⁵ indicate? | 9 |
| ¹⁶ reference sec in r&d chap | 11 |
| ¹⁷ ref? | 12 |
| ¹⁸ by 'address' do you mean make it longer? | 12 |
| ¹⁹ opaque? | 13 |
| ²⁰ what? the fiber bundles? | 13 |
| ²¹ signals coming from wire wrapping? How about 'signals coming from wires on the | |
| ²² APA frames'? | 14 |
| ²³ ref section | 14 |
| ²⁴ Do we say 'a sipm' or 'sipm technology'? Plain 'sipm' sounds funny. | 14 |
| ²⁵ 'linearity range' means linearity over range of wavelengths? Plz clarify | 14 |
| ²⁶ operates like a geiger counter? I'd say, either give a more complete description of | |
| ²⁷ how they work or leave this off. Feels like it's out of the blue. Just MHO. AH | 15 |
| ²⁸ but not the models already tested? Clarify (per the below) | 16 |
| ²⁹ so the 'follow-up' tests were done on these new models? | 16 |
| ³⁰ Do we need prev sentence? | 16 |

| | | |
|----|---|----|
| 1 | Can we summarize the current status? Which model is in the lead? | 16 |
| 2 | Make sure PD always refers to the whole thing not just the sippm | 18 |
| 3 | ref? | 18 |
| 4 | 'in the last ...' might be very recent. "In the last couple or few months?" | 18 |
| 5 | tests produced a device? Plz clarify | 18 |
| 6 | This pgraph is confusing | 18 |
| 7 | do we need prev (...)? | 20 |
| 8 | this seems wrong, plz check | 21 |
| 9 | Is this in the running? If not, leave out. If so, why not mentioned till now? | 23 |
| 10 | devices of the 3 technologies are packaged together and the package is mounted on the apa? or the three all use the same mounting features? I'm confused | 23 |
| 1 | reference? | 23 |
| 2 | reference? | 24 |
| 3 | constraints? | 24 |
| 4 | Something about how this is still better than installing them after wire-wrapping; list a risk or two of that method, maybe, for comparison | 24 |
| 5 | figure could use labeling | 24 |
| 6 | I can't parse this phrase | 25 |
| 7 | | 25 |
| 8 | what's cddf? | 25 |
| 9 | | 25 |
| 10 | ? | 25 |
| 11 | ? | 29 |
| 12 | check ref | 29 |
| 13 | check ref | 29 |
| 14 | of Ar atoms? | 29 |
| 15 | can you be a bit more specific? | 29 |
| 16 | | 29 |
| 1 | | 29 |
| 2 | | 30 |
| 3 | No fig1 exists for: Block diagram of the photon detector signal processing system. | 30 |
| 4 | not 'is'? | 30 |
| 5 | if it's a pair, is it just dual-conductor? This is confusing | 31 |
| 6 | has been found to be? | 31 |
| 7 | | 31 |
| 8 | outputs? | 31 |
| 9 | get number | 31 |
| 10 | | 32 |

| | | |
|----|--|----|
| 11 | There's that 'generally' again! | 32 |
| 12 | not full sentence | 34 |
| 13 | | 34 |
| 14 | 'the' makes it sound like we've heard of the microzed thing, but we haven't yet | 35 |
| 15 | "The module also features charge injection for performing diagnostics, linearity monitoring and voltage monitoring. " or "The module also features charge injection for performing diagnostics and linearity monitoring, and it also features voltage monitoring. "? | 35 |
| 19 | Start with a sentence that says what alternatives this section discusses: CE, pulse-shaping, ASIC... | 35 |
| 21 | | 35 |
| 22 | check | 35 |
| 23 | prev sentence unclear. what depends on no. of channels? | 36 |
| 24 | I'm not sure I got this right; I didn't completely understand the orig sentence to begin with | 36 |
| 26 | check | 36 |
| 27 | reducing speed of readout links is a virtue? | 37 |
| 28 | how does large channel count relate to reduction in cost? | 37 |
| 29 | connect direct digitization with ASIC | 37 |
| 30 | | 38 |
| 1 | fix | 38 |
| 2 | what's N2? | 38 |
| 3 | 'is planned...'? | 38 |
| 4 | 35t calibration? | 39 |
| 5 | that's a mouthful | 42 |
| 6 | give section | 43 |
| 7 | | 43 |
| 8 | | 44 |

⁹ Chapter 1

¹⁰ Photon Detector

ch:photon

¹¹ 1.1 Introduction

In our 2012 CDR we started each chapter with: The scope of the (whichever) subsystem includes the design, procurement, fabrication, testing, delivery and installation of the mechanical and high voltage components of the (blah); followed by list of components – see the TPC chapter. At this late date, not sure it's worth it...

¹² Liquid argon is an excellent scintillating medium. With an average energy needed
¹³ to produce a photon of 19.5 eV (at zero field) a typical particle depositing 1 MeV in
¹⁴ liquid argon will generate 40,000 photons with wavelength of 128 nm. At higher fields
¹⁵ this will be reduced but at 500 V/cm the yield is still about \sim 20,000 photons per
¹⁶ MeV. Roughly 1/3 of the photons are promptly emitted after about 6 ns while the
¹⁷ rest are emitted with a delay of 1100-1600 ns. LAr is highly transparent to the
¹⁸ 128 VUV photons with a Rayleigh scattering length and absorption length of 95 cm
¹⁹ and >200 cm respectively. The relatively large light yield makes the scintillation
²⁰ process an excellent candidate for determination of t_0 for non-beam related events.
¹ Detection of the scintillation light may also be helpful in background rejection.

³ 1.2 Requirements and Goals

⁴ 1.2.1 Beam-based physics

⁵ There are no requirements for the beam-based physics program, as the machine clock
⁶ will provide a t_0 with roughly 10 μ s resolution. Given that the electron drift is 1.6

7 mm/ μ s the uncertainty to the electron lifetime correction is small is
8 when?

9 the beam timing is used. The photon system can be useful in determining the t_0
10 of cosmic ray events and events from radiological decays as well as giving a handle to
11 the location of beam events in the LAr volume with respect to fiducial boundaries.
12 The impact of the LAr scintillation light on the detector performance needs to be de-
13 termined, but it is not expected that the reduction in backgrounds for the oscillation
14 program will introduce additional requirements to the photon system design.

15 **1.2.2 Proton Decay and Atmospheric Physics**

16 The photon detector system must provide the t_0 for non-beam related physics chan-
1 nels if a correction for electron recombination during drift is to be applied. The
2 requirements for electronics and hadronic energy resolution for the proton decay and
3 the atmospheric neutrino program are $1\%/\sqrt{E(\text{GeV})} \oplus 1\%$ and $30\%/\sqrt{E(\text{GeV})}$ re-
4 spectively. With these resolutions the collected charge must be accurately corrected
5 for recombination. Therefore the photon system must provide a t_0 for particles with
6 >100 MeV with >95% efficiency in the fiducial volume of the detector.

7 **1.2.3 Low-energy Physics**

8 Supernova events will produce neutrinos down to about ~5 MeV. Studies have es-
9 timated the momentum resolution for 5 MeV electrons to be 20% using only TPC
10 information and assuming a highly efficient trigger and an electron lifetime of 5 ms.
11 The impact of various detector resolutions on the physics potential of LBNE has not
12 been studied in detail. At present there is no strong requirement that the energy
13 resolution be better than 20%, so no requirement on the photon system trigger effi-
14 ciency is set at this time. However it is clear that if a detector design can be found,

15 clarify ‘detector design can be found’
16

17 the energy resolution would greatly improve. A goal of the photon detection
18 R&D is to develop a system with the lowest possible threshold for a reasonable cost.
19 At the start of final design, a final decision as to the configuration will need to be
20 made based on cost and added physics capability.

21 1.2.4 Required Performance

22 To achieve the physics goals in the previous section the performance of the photon
 23 detection system must be understood. The prototype readout electronics described
 24 in Section 1.6 have been shown to detect the single photoelectron (p.e.) signals
 25 associated with the late scintillation light but future versions may sacrifice this ability
 26 to mitigate high channel costs. It is assumed that the physics goals of the photon
 1 detection system will be met using the prompt scintillation light.

2 The performance, or overall photon collection efficiency, is given by the following,
 3 where it is assumed only prompt light is collected:

$$\frac{N_{pe}}{MeV} = N_{128} \cdot \epsilon_{geom} \cdot \epsilon_E \cdot \epsilon_{mesh} \cdot \epsilon_{conv} \cdot \epsilon_{capt} \epsilon_{tran} \cdot \epsilon_{QE} \quad (1.1)$$

4 The efficiencies leading to the overall number of photo-electrons collected by the
 5 photon detection system, $\frac{N_{pe}}{MeV}$, are given in table [Table-Eff](#).

Table 1.1: Individual photon collection efficiencies

| Factor | Description | Value | Comments |
|-------------------|------------------------|---------------|---|
| ϵ_{geom} | geometric acceptance | 0.0036 | historical average |
| ϵ_E | field correction | 0.6 | 500 V/cm |
| ϵ_{mesh} | TPC wire shadowing | .83 (30-150°) | HimmelMesh falls off sharply [?] |
| ϵ_{conv} | TPB conversion | 1 | bib:gehrman see ref. [?] |
| ϵ_{capt} | waveguide incident | 0.5 | about half converted photons travel into waveguide |
| ϵ_{tran} | waveguide transmission | TBD | prototype dependent |
| ϵ_{QE} | SiPM QE | .31 | SensL b-series |

6 Using Equation 1.1 it is seen that to detect a 2 p.e. signal, likely to be dis-
 7 criminated from noise, the transport efficiency is 1.2%. Of course this value is very
 8 position-dependent, as the geometric acceptance, wire shadowing and transport cor-
 9 rections all depend on the location of the event. Figure [fig:photon_map](#) shows the probability of
 10 (?)

11 MeV energy deposition being detected in the photon detectors.

13 The TPC wire mesh shadowing is also quite location-dependent as photon an-
 14 gles, relative to the wire plane, lead to rapid loss in transmission below 30° and

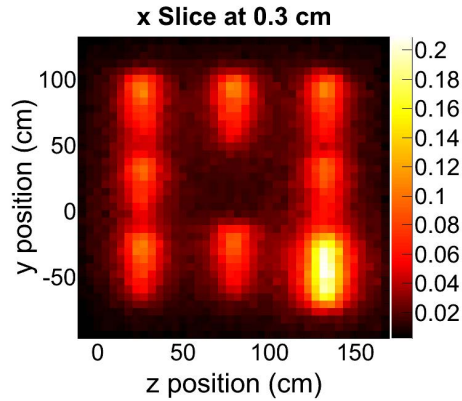


Figure 1.1: Photon map giving the probability of photon being detected in the photon detectors when depositing energy at map location.

(need general TPC cell map with better description)

`fig:photon_map`

15 greater than 150° . Lastly, the photon detector paddles themselves can have position-
 16 dependent response to incident photons due to the attenuation length of the waveg-
 17 uide. The photon detector simulation, which is nearing stable operation, will be able
 18 to better estimate the efficiencies coming from geometric acceptance correction.

19 1.2.5 General Considerations

20 In the event that higher photon collection efficiencies can be achieved it should be
 21 possible to improve the energy resolution of the detector by adding the photon yield
 22 to the electron yield information. However this requires several orders of improve-
 23 ment in light collection efficiency, so it is beyond the scope of the present design.

24 1.3 Photon Detector Prototype Designs

25 All designs considered for the photon detector have been based on the use of wavelength-
 26 shifting coating, or bulk doping, of plastic materials coupled to silicon photomulti-
 27 pliers (SiPMs). The reference design utilizes a coated acrylic waveguide coupled
 28 to SiPMs. This waveguide is described in Section 1.3.1. Alternate waveguide de-
 29 signs, described in the following sections, have been developed in an effort to optimize
 30 coverage, cost and attenuation length.

1.3.1 Cast or Bulk Doped Acrylic Bars

¹ sec_bars
² The reference design for the photon detection system is based on light guides that
³ are coated with wavelength shifter. The 128-nm scintillation photons from liquid
⁴ argon interact with the wavelength shifter on the light guide surface and 430-nm
⁵ light is re-emitted in the bar. The light guide channels the light to photodetectors
⁶ at its end.

⁷ A schematic drawing of a light guide with its photosensors is shown in Figure 1.2.
⁸ The prototype light guides are bars with a footprint 2.54 cm × 0.6 cm. The concept
⁹ is described in Ref. [?].

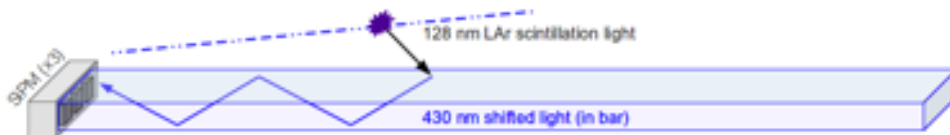


Figure 1.2: Schematic drawing of a light guide with its photosensors. The bars have embedded wavelength shifter (WLS), either TPB or bis-MSB. Three SiPMs collect the waveshifted photons that have been internally reflected to the bar’s end.

Fuzzy at this size

¹⁰ The wavelength shifter converts incident VUV scintillation photons to 430 nm
¹¹ photons inside the bar, with an efficiency of $\sim 50\%$ for converting a VUV to an opti-
¹² cal photon [?]. A fraction of the waveshifted optical photons are internally reflected
¹³ to the bar’s end where they are detected by SiPMs whose QE is well matched to
¹⁴ the 430-nm waveshifted photons. The light guides were made with one of two wave-
¹⁵ length shifters: the conventional TPB (1,1,4,4-tetraphenyl-1,3-butadiene) and the
¹⁶ less expensive alternative bis-MSB (1,4-bis-(o-methyl-styryl)-benzene). Preliminary
¹⁷ studies with a VUV monochromator show that the two wavelength shifters compare
¹⁸ favorably in their waveshifting efficiency [?]. A testing program is currently underway
¹⁹ to compare their relative performance in liquid argon.

²⁰ A team at Indiana University is studying prototype light guides made with three
²¹ different technologies. These technologies are listed in Table 1.2.

²² The clear acrylic bars (a) are made from blanks of commercially available Lucite-
²³ UTRAN cast UVT acrylic sheet that has been laser-cut and diamond-polished into
²⁴ bars of the proper size. Lucite-UTRAN has the longest attenuation length of the
²⁵ acrylics tested [?]. The Eljen¹ bars (b and c) are commercial light guides that
²⁶ are doped with J2 green fluor (equivalent to Y11). Two types of light guides were

¹<http://www.eljentechnology.com>

Table 1.2: Light guide technologies

| Label | Light Guide Technologies |
|-------|---|
| (a) | clear acrylic, dip-coated |
| (b) | doped Eljen PVT light guide, dip-coated |
| (c) | doped Eljen polystyrene light guide, dip-coated |

ab:lightGuides

27 purchased from Eljen. The light guides (b) were fabricated from polyvinyl toluene
 28 (PVT); these are the standard Eljen product EJ-280. The quantum efficiency of
 29 the fluorescent dopant in EJ-280 is 0.86, so the second shift in wavelength does not
 30 markedly degrade the photon detector efficiency. The light guides (c) were fabricated
 31 from polystyrene; these light guides were ordered because PVT bars can craze if
 32 cooled too rapidly. Although the PVT light guides may be brighter, no instance of
 33 crazing has ever been observed in polystyrene light guides.

1 For the acrylic light guides, the WLS must be embedded in the plastic at the
 2 bar's surface so that 128-nm scintillation photons can generate optical 430-nm pho-
 3 tons within the volume of the plastic. Otherwise the VUV photons will not be
 4 trapped by the light guide. For the Eljen bars, the wavelength shifter can either be
 5 embedded in the plastic, as with the acrylic, or it can be deposited on a plate or
 6 film placed in proximity to the light guides. The J2 wavelength shifter then converts
 7 the resulting 430-nm photons inside the light guides where they are channeled to the
 8 photodetectors.

9 To embed the WLS at the surface of the light guides, a “dip-coating” process was
 10 developed at Indiana University. Before the WLS was applied to the acrylic bars,
 11 the bars were annealed at 80°C for one hour. (The Eljen bars were not annealed.)
 12 The WLS was dissolved in the organic solvent dichlormethane (CH_2Cl_2). For these
 13 waveguides 5 g of wavelength shifter was dissolved in 1,000 gm of DCM. A series of
 14 experiments showed that this concentration was optimum. A bar was first dipped
 15 into the WLS mixture for 15 seconds and then removed. It was then hung in the dark
 16 for at least two hours to dry. Once dry, the ends of the bars were flycut. Currently
 17 designs are being fabricated that put an acrylic plate painted with WLS or a thin
 18 film impregnated with WLS in front of the Eljen light guides.

19 In summer 2015 these designs will all be tested side-by-side at the TallBo dewar
 20 facility at Fermilab under uniform, low-contamination conditions. In addition to
 21 the designs described above, these tests will include photon detector designs from
 22 Colorado State University and Louisiana State University. This experiment will
 23 compare the relative performance and the absolute efficiency for all designs scaled

²⁴ to 1.5 m.

²⁵ 1.3.2 Fiber-embedded Bulk Acrylic Plate

²⁶ The LSU team has developed a VUV photon detector design for a large LAr detector
²⁷ that overcomes some of the shortcomings of the present LBNE baseline
²⁸ define ‘baseline’ here; do you mean ‘reference design’?

²⁹ photon detectors. The LSU photon detector design allows for coverage of a very
³⁰ large area, thereby increasing the geometrical acceptance of the photon detectors.
³¹ The number of required SiPMs and readout channels per unit detector area covered
³² with photon detection panels has been significantly reduced to keep the overall cost
³³ for the photon detection system at or below the present design while increasing the
³⁴ geometrical acceptance.

³⁵ The photon detection system consists of a TPB-coated acrylic panel with an
¹ embedded S-shaped wavelength shifting (WLS) fiber. The fiber is read out by two
² SiPMs, which are coupled to either end of the fiber, and serves to transport the
³ light over long distances with minimal attenuation. The double-ended fiber readout
⁴ has the added benefit of providing some position dependence to the light generation
⁵ along the panel by comparing relative signal sizes and arrival times in the two SiPMs.
⁶ Figure 1.3 shows a drawing of the layout and a photograph of a prototype photon
⁷ detection panel in the test stand at LSU. The incoming 128-nm VUV Ar scintillation
⁸ light will be converted by the thin TPB layer on the acrylic panel and re-emitted
⁹ with wavelength peaking at 430 nm in an isotropic way. About 50% of the light is
¹⁰ emitted into the acrylic panel where some fraction will be absorbed by the WLS fiber
¹¹ and converted to light with a peak intensity of about 480 – 500 nm. The green light
¹² exiting the fiber is well matched to the peak photon detection efficiency of typical
¹³ SiPMs.

¹⁴ 1.3.3 LSU Photon detection panel production

¹⁵ The photon detection panels are produced from 0.25-inch-thick sheet UVT acrylic
¹⁶ and cut to size. For a first series of prototypes the acrylic panel dimensions were
¹⁷ chosen to closely match the area of four bars of the LBNE baseline
¹⁸ reference?

¹⁹ photon detection system. The groove is cut with a CNC mill in several passes to
²⁰ achieve good groove surface quality, which is important for good light transmission
²¹ from the bulk acrylic to the fiber. The panels are dip coated with TPB and left to dry

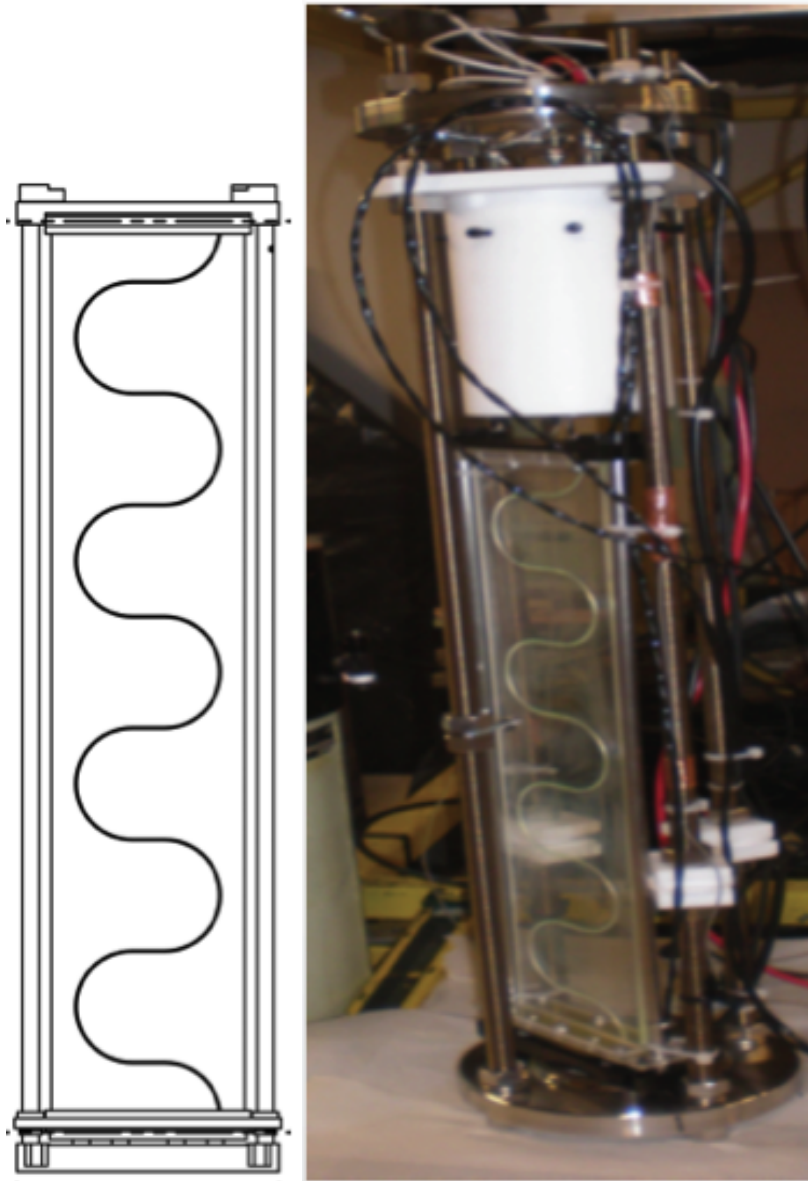


Figure 1.3: LSU photon-detection panel. Technical drawing of a $20'' \times 4.33''$ acrylic panel with embedded WLS fiber (left) and picture of a prototype in test set-up at LSU (right) with the same dimensions.

fig:1-LSU

1 prior to insertion of the WLS fiber. Panels with two and three layers of fibers inserted
2 and glued into the groove have been produced. Fiber ends are cut and polished. The
3 resulting acrylic panels are then inserted into a custom-made mechanical frame. The
4 end caps of the mechanical frame house one SiPM on either end. The presently used
5 $6 \times 6\text{mm}^2$ active-area SiPMs are spring-mounted to ensure good contact between the
6 active area and the fiber ends. The leads of the SiPMs are connected to a small PCB
7

8 **define**

9 onto which $\sim 2\text{-m}$ -long twisted-pair coax cables are soldered to supply the SiPM
10 with a bias voltage and to read out signals. The other cable ends are typically
11 connected to pre-amplifiers before leading to a DAQ system. Components for the
12 photon detection panels are inspected at all stages of the manufacturing process for
13 quality. Due to the small number of panels produced to date, no quantitative quality
14 control parameters have been defined yet. Proper connectivity of the fully assembled
15 units are tested in a setup at LSU using a LED flasher. If LED light signals are
16 seen, the panel is successively immersed in gaseous argon (GAr) along with an alpha
17 source. The observation of scintillation light originating from alpha particles and
18 cosmic rays penetrating the GAr volume allows for a relatively quick quality-control
19 check of a completed photon detector at room temperature.

20 **1.3.4 Proof-of-Concept and Prototype Detector Results**

21 Several photon detector panels of $20 \times 4.33\text{in}^2$ have been produced and two have
1 been tested in a LAr test stand at CSU. The detectors submitted to the cold test
2 have three and two embedded fibers, respectively, but are otherwise produced in the
3 same way. The data taken in LAr included self-triggered alpha source scans as well
4 as cosmic runs with a muon hodoscope providing a trigger for near-vertical muons
5 penetrating the LAr volume.

6 **Alpha source runs:** The alpha source was placed at a distance of about 1 inch
7 in front of the center line of the photon panel and moved to 20 different positions
8 spaced about 1 inch apart from neighboring positions. At each position 5000 signal
9 traces were recorded and measurements were repeated for three of the positions to
10 check the reproducibility of the measured light yield. Figure 1.4 shows results for
11 both successively measured panels. The red and blue dots show the mean light yield
12 values in units of p.e. (photo electron equivalents = no. of fired SiPM pixels) for the
13 SiPM on the top and bottom end of the panel as function of source position. Green
14 dots show the sum of both channels. The summed signals provide

Fig 1.4 - LSU

indicate?

a very uniform detector response for the entire panel, independent of the alpha source position. The data also indicate good reproducibility for the doubly measured positions. The three-fiber panel shows about 50% more light when compared to the two-fiber panel, which is in good agreement with expectations. It needs to be pointed out that the LAr purity was not monitored and that measurements for the two panels were performed sequentially after refilling the dewar with LAr. However, the liquid argon for both measurements came from the same batch, which motivates the assumption that the purity for both measurements was very similar.

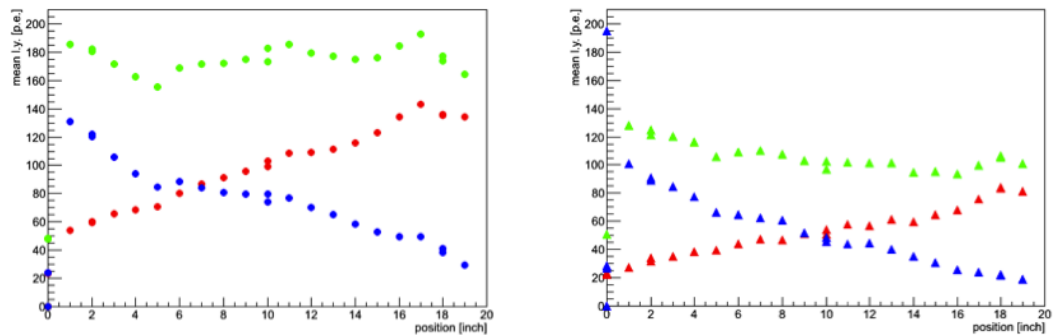


Figure 1.4: Light yield for the three (left) and two (right) fiber LSU photon detection panels in response to a 1-in distant alpha source in LAr. Red and blue symbols represent the mean light yield over 5000 trigger events from a single SiPM each and green points represent the summed signal from both SiPMs.

fig:2-LSU

Cosmic trigger runs: Two $1'' \times 10''$ wide scintillator counters were placed above and below the dewar to form a muon hodoscope and to select near-vertical muons traversing the LAr volume. The three-fiber LSU panel and one LBNL/Elgin Bis-MSB doped polystyrene bar of LBNE baseline dimensions and read out by three SiPMs were simultaneously inserted in the LAr. The setup allowed the study of the response of these photon detectors to scintillation light created by penetrating cosmic muons. A detailed quantitative comparison of the relative light yield was not possible with this setup due to large systematic uncertainties in the position dependence of the scintillation light generation by the triggering cosmic muons. A qualitative comparison of the detector responses, taken as the signal sum of three and two SiPMs for the Elgin bar and the LSU panel, respectively, shows comparable light yields as shown in Figure 1.5.

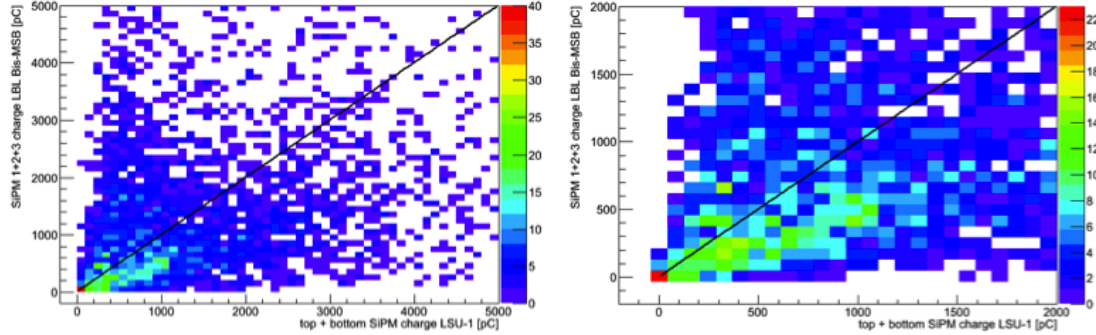


Figure 1.5: Scatter plot of the summed charge of three SiPMs coupled to the LBNL/Elgin Bis-MSB doped bar and the summed charge of two SiPMs for the three-fiber LSU panel in response to an external muon hodoscope trigger. The right plot shows a zoomed version of the left plot.

fig:3-LSU

1.3.5 R&D Work in Progress and Present Plans

After the construction and proof-of-principle test of the LSU-style photon detection panels several 2.17-m-long and 110-mm-wide (=4.33") panels were manufactured to demonstrate the scalability of the design. At the time of writing, tests in the large LAr dewar at CSU are in progress. The team is performing alpha source scans and cosmic muon runs. The alpha source scan runs are arranged such that the source illuminates two photon detectors at the same time. This setup facilitates quantitative and relative light yield comparison between different photon detector designs in the same LAr bath with a well-defined VUV light source.

Manufacturing and testing of wider panels is under consideration to maximize the photon detector panel area in the DUNE LAr far detector. The goal is to cover the entire anode plane assembly (APA) area with photon detectors embedded into the APA frame. Another important measurement goal is to establish the energy threshold of the photon detection panels. A study will be conducted for the photon detectors presently installed in the 35t detector

reference sec in r&d chap

using Michel electrons. The 35t detector contains one of the three-fiber LSU photon detection panels. In addition, performing alpha source runs in a well-controlled and monitored LAr setup may provide information on the particle energy threshold for observation of VUV scintillation light. The measurement of a photon detector panel's light yield as function of the source distance is another key measurement to

5 estimate the response and sensitivity of the full photon detection system in a LAr
6 detector. Results will be useful to validate MC simulations. We are exploring options
7 to perform these tests in the large dewar setup at CSU or alternatively in the TallBo
8 setup

9 ref?

10 at FNAL.

11 The TPB coating procedure of the acrylic panels has not yet been optimized and
12 improvements may be possible. A systematic study is foreseen to identify parameters
13 in the TPB dip and in the evaporation coating procedure to maximize the light yield
14 of resulting samples. These tests will be performed on small $10 \times 10 \text{ cm}^2$ acrylic
15 panels with a U-shaped embedded WLS fiber. On the software and analysis side,
16 tools are being improved to study position dependence for alpha-source run data
17 using relative signal timing and size. Furthermore, it is planned to continue work on
18 analysis algorithms to identify the late light component from argon scintillation.

19 Finally, early exploratory work on wallpapering the TPC cathode planes with
20 TPB coated Tetratex foils and observing the shifted light with suitably installed
21 photon sensors in combination with light collector cones will be pursued and explored
22 more rigorously to provide timely results.

23 1.3.6 Fiber Bundle with WS-coated Radiator

24 A reduction in attenuation length has been observed in acrylic waveguides that have
25 been doped with TPB. One possible way to address this reduction would be to
26 populate the PD system with half-length paddles. However, this would lead to an
27 increase in the number of readout channels, and readout electronics is the driving
28 cost of the photon detector system. While it may be possible to combine readout
29 channels to mitigate the increase in overall number, a more desirable solution would
30 be to address the attenuation length issue.

1 by ‘address’ do you mean make it longer?

2 To mitigate the reduced attenuation length in TPB-doped or -coated acrylic and
3 polystyrene, the CSU group has been developing an alternative design based on UV-
4 to-blue wavelength shifting fiber (Y11) that has not been treated with TPB. A thin
5 TPB-coated acrylic radiator located in front of a close-packed array of WLS fibers.
6 Figure 1.6 shows a photograph of the fiber-bundle prototype.

7 The VUV photons are incident on the TPB-coated plastic radiator and roughly
8 half of the photons converted in the radiator are incident on the fiber bundle. These
9 photons are then directed onto SiPMs at one end. The Y11 fiber (from Kuraray



Figure 1.6: Photograph of fiber-bundle PD prototype (early one-sided version). The thin TPB-coated radiator is mounted on top of the prototype in the image.

fig:fiber_bund

10) have mean absorption and emission wavelengths of about 440 nm and 480 nm
11 respectively. The attenuation length of the Y11 fibers is given to be greater than
12 3.5 m at the mean emission wavelength, which allows production of full-scale (2.2-m
13 length) photon detector paddles.

14 First prototypes of this design utilized two rows of fibers with a reflector behind
15 the double row used to redirect the unabsorbed \sim 400 nm photons back through the
16 two rows. Data taken at the CSU Cryogenic Detector Development Facility (CDDF)
17 and the Fall 2014 FNAL Tallbo test showed that the front row of fibers collected
18 twice as much light as the back row, thus only a single row design can be considered
19 — this is currently under development. The current design utilizes two single rows
20 of fibers back-to-back with layers of

21 opaque?

22 Tyvek diffuse reflector between them.

23 In this design

24 what? the fiber bundles?

25 would face into different TPC cells, allowing additional information to be used
26 in the disambiguation of the TPC signals coming from wire wrapping on the APA

²⁷ frames.

²⁸ signals coming from wire wrapping? How about ‘signals coming from wires on the APA frames’?

¹ If the walls of the detector were to be covered with TPB-coated material shifting
² the VUV photon to blue, the WS-fiber in this design could capture the emitted
³ light, offering a further benefit. Further study is required to determine the effect
⁴ these enhancements would have on the physics reach of the detector.

⁵ To fully exploit this approach several design optimizations need to be examined,
⁶ including the following:

- ⁷ • TPB coating thickness on thin radiator
- ⁸ • Double-ended readout; if the fibers are read out from both ends and the corre-
⁹ sponding channels are ganged onto one readout channel, an increase in channel
¹⁰ output can be obtained without significant cost
- ¹¹ • Use of custom-doped fibers to best match the QE response of the SiPMs and
¹² the emission spectrum of the TPB
- ¹³ • Removal of the radiator and coating the TPB directly onto the outer fiber-
¹⁴ cladding of the Y11 fibers. Since the fibers are double-clad it may be the case
¹⁵ that the attenuation length of the fibers is not altered by the TPB applica-
¹⁶ tion. The geometry of the close-packed fiber row may lead to increased photon
¹⁷ (400 nm) collection

¹⁸ The cost of this design is comparable to that of the bar-based design but is slightly
¹⁹ more complex to fabricate — although the Y11 fibers are commercially available,
²⁰ which is an attractive feature. The engineering aspects of the design will be discussed
²¹ in the appropriate section of this chapter.

²² ref section

²³ 1.4 Silicon Photomultipliers

²⁴ Silicon Photomultipliers (SiPMs) have been selected as the reference design photon
²⁵ detectors for the far detector LArTPC.

²⁶ Do we say ‘a sipm’ or ‘sipm technology’? Plain ‘sipm’ sounds funny.

²⁷ A SiPM is a photo detection device sensitive to single photons with excellent
²⁸ linearity range

29 ‘linearity range’ means linearity over range of wavelengths? Plz clarify

30 in collecting multiple photons. A SiPM consists of a large avalanche photodiode
31 (APD) array built on a common silicon substrate. APDs operate in Geiger mode.

32 operates like a geiger counter? I'd say, either give a more complete description of
33 how they work or leave this off. Feels like it's out of the blue. Just MHO. AH

33 SiPMs have been developing at a very fast pace in recent years, in response to the
34 needs of the medical industry. As a result, the price of SiPMs has gone down, while
1 their performance has greatly improved. A number of characteristics make SiPMs
2 an attractive choice as photon detectors for the PD system:

- 3 • High photon-detection efficiency (PDE), up to 40-50% at the peak detection
4 wavelength.
- 5 • High intrinsic gain ranging from 10⁵ to 10⁷ depending on the overvoltage
- 6 • Low dark rate at cryogenic temperatures — less than 50 Hz even at the maxi-
7 mum overvoltage
- 8 • Insensitivity to external magnetic field
- 9 • Extremely linear gain vs. overvoltage
- 10 • Low cost per sensitive area compared to small cryogenic photomultiplier tubes
11 (PMTs)
- 12 • Small dimensions allowing a simple, compact and robust design
- 13 • No need for high voltage (HV) power.
- 14 • Low bias voltage, typically less than 100 V required, and even less than 30 V
15 in some cases, resulting in low peripheral costs
- 16 • Maintenance of high gain and PDE at cryogenic temperatures

17 In short, SiPMs have demonstrated performance comparable to traditional PMTs,
18 but at a significantly reduced cost and are the photon-detector of choice for PD
19 system of the far LArTPC detector.

20 The main risk associated with using SiPMs is operation at LAr temperature.
21 SiPM data sheets neither show nor guarantee the device's performance at cryogenic
22 temperatures. Most of the low-temperature tests performed by LBNE teams on

23 SiPMs in the last two years have been done using LN2, as it has similar temperature
24 (10 K below LAr) but costs much less.

25 A number of SiPM manufacturers offer SiPMs, such as SenSL, Hamamatsu,
26 KETEK, AdvanSiD, CPTA (Photonique), Philipis, Novel Device Laboratory (NDL),
27 Zecotek, Voxtel, Amlification Technologies, Excelites, but only a fraction of them of-
28 fer SiPMs suitable for the PD system — large area ($6 \times 6\text{mm}^2$ or $3 \times 3\text{mm}^2$), large fill
29 factor, pin or surface mount and no housing. An exhaustive search of suitable SiPMs
30 was conducted in 2012 and sample SiPMs were obtained from SenSL, Hamamatsu,
31 CPTA and AdvanSID. It should be noted, however, that new, improved models
32 appear every year from most manufacturers.

33 The initial round of tests included models from SenSL (MicroSM-600-35-X13),
34 Hamamatsu(MPPC S10985-100C), CPTA (SSPM-0710G9MM) and AdvanSID (ASD-
1 SiPM3S-P). In this test, SiPMs were cooled in liquid nitrogen, laser light pulses at
2 400 nm wavelength were used as the light source and signal output as a function of
3 overvoltage was recorded. Results can be seen in Figure ??.

4 Based on these initial tests and high price quotes received at the time from
5 AdvanSiD and CPTA, the follow-up tests focused on SenSL and Hamamatsu models.
6

7 but not the models already tested? Clarify (per the below)

8 Shortly after initial tests, SenSL came up with a new model (MicroFB-600-35-
9 SMT followed by improved MicroFC-600-35-SMT) and most of the tests

10 so the ‘follow-up’ tests were done on these new models?

11 have been done on the SenSL models. Hamamatsu’s MPPC S12895- 0404-
12 PB50 has been on the market for a long time and Indiana group measured very high
13 cross-talk and afterpulsing rates.

14 Do we need prev sentence?

15 Hamamatsu released a new, improved model in 2015, S13360, that will be tested
16 in 2015 and compared with SenSL models.

17 Can we summarize the current status? Which model is in the lead?

18 **1.4.1 Requirements**

1 Despite argon’s excellent scintillation yield, the PD system requires high-sensitivity
2 photon detectors due to the very small surface area of the SiPMs. Furthermore, the
3 late scintillation light in argon represents 2/3 of the total, but it is spread over 1100
4 – 1600 ns, making the individual late-light signals very small on average.

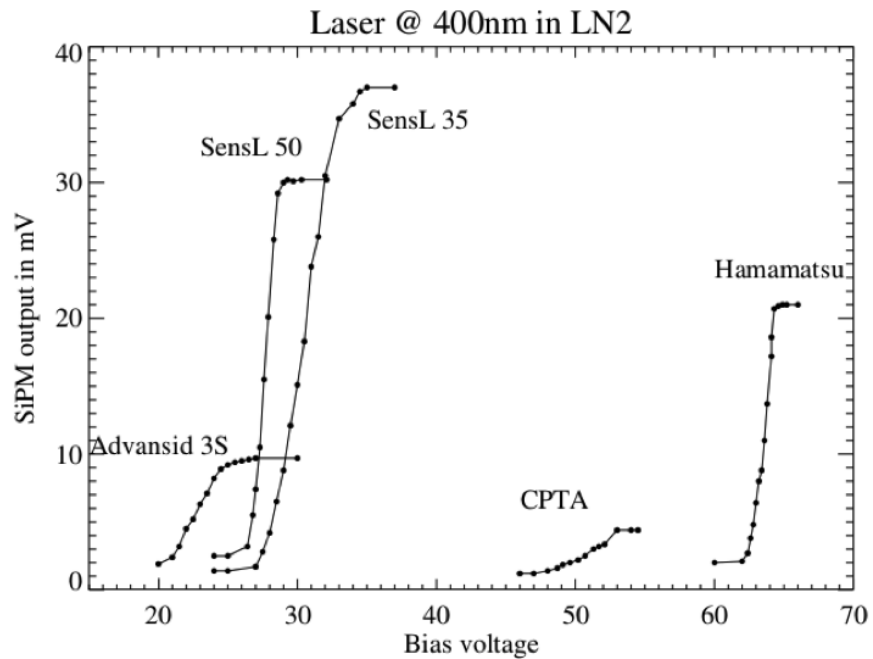


Figure 1.7: SiPM signals as function of bias voltage in liquid nitrogen. Liquid nitrogen has 10 K lower temperature than liquid argon, making the measurement applicable. In all cases there is a significant increase in gain with increasing bias voltage, but difference in gain among different samples is clearly visible.

fig:laser400

5 SiPM data sheets indicate that these requirements are satisfied, but it is important
6 to observe similar performance at LAr temperatures in terms of high gain,
7 sensitivity to single photoelectrons, high PDE, linearity of response, stability of
8 breakdown voltage, long-term stability, low afterpulsing and low cross-talk. In addition,
9 SiPMs must exhibit mechanical robustness and low dark rate as they undergo
10 cryogenic cooling and cycling. Finally, the cost must be low enough. To avoid sole-
11 sourcing, it is required to identify at least two choices that meet all the requirements.

12 Institutions designing different PD prototypes (IU, CSU and LSU) have conducted a number of tests of PDs with SiPMs.

13 Make sure PD always refers to the whole thing not just the sipm

14 Additional, specifically targeted tests have been conducted at LSU and University
15 of Hawaii (UH) in recent months. The parallel tests conducted at LSU and UH will
16 ensure important cross-checks and reduce possible testing biases — this is important
17 for selecting the best photo-sensors.

19 1.4.2 Test Results

1 In the last 18 months, a test setup for SiPM evaluation has been built, that includes
2 Belle experiment

3 ref?

4 electronics to power and record signals from SiPMs. More recently

5 ‘in the last ...’ might be very recent. “In the last couple or few months?”

6 , a new board similar to the SenSL testing board has been designed to address
7 noise problems and low amplification found on the Belle board, issues that become
8 critical at low light levels. This new board is currently being used to conduct dark
9 rate and single-photoelectron studies. Figure ?? shows the layout of this board and
10 a picture of the actual circuit as built.

11 As previously mentioned, tests focused on Hamamatsu and SenSL produced 8
12 SiPMs.

13 tests produced a device? Plz clarify

14 However, the IU group found out that Hamamatsu SiPMs are placed in a dewar
15 inside a copper plated dark box and cooled with LN2. SiPMs are held in place on
16 the PCB with acrylic holder as shown in the Fig ??.

17 This pgraph is confusing

18 Different contraction rates of materials in LN₂ produced mechanical damage to
1 some of the SiPMs. To address this issue, a PCB board with spring-loaded POGO

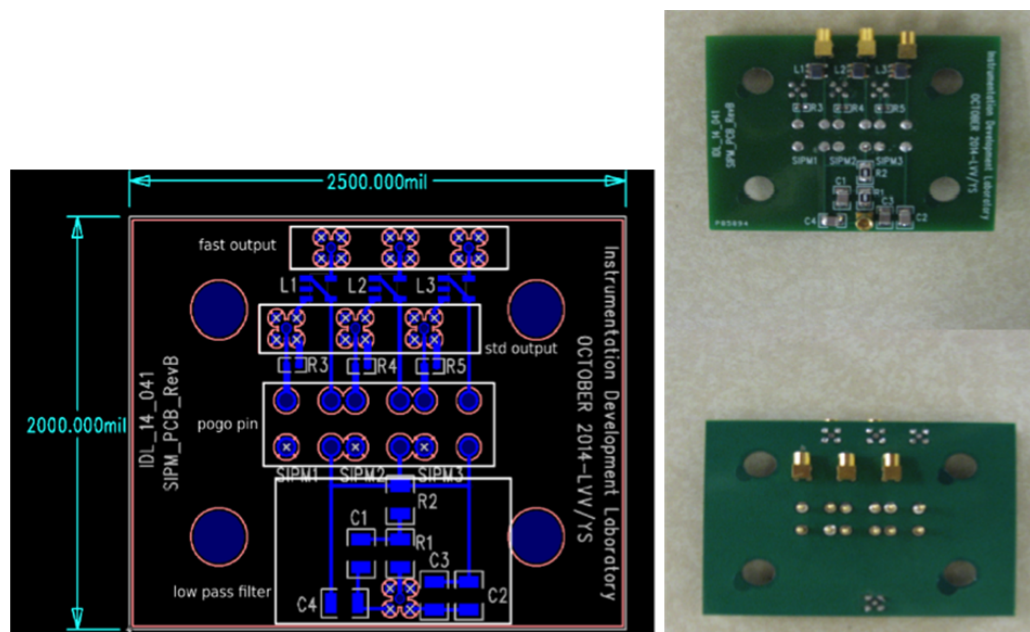


Figure 1.8: The diagram on the left shows the schematics of the PCB board. The picture on the right shows the PCB as built. This PCB can accommodate three SiPMs for testing.

fig:sipm_schem

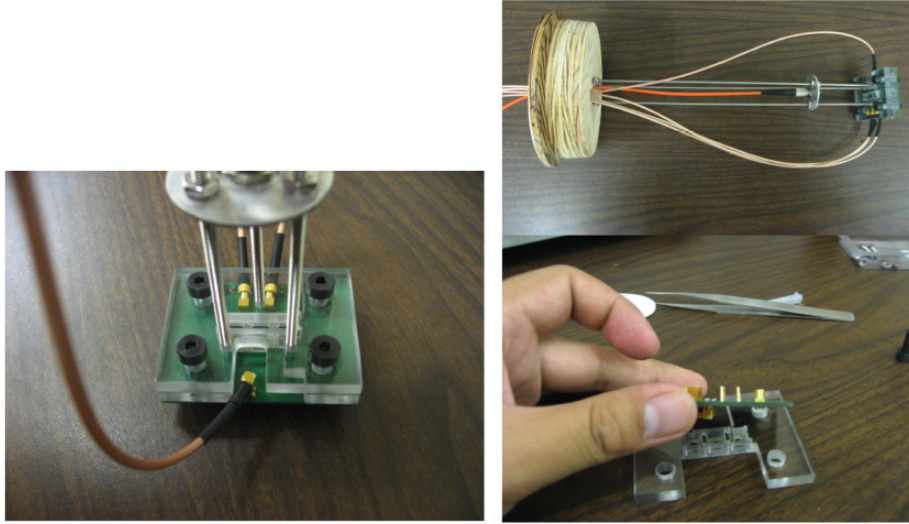


Figure 1.9: Picture on the left shows acrylic holder that secures SiPMs to the PCB while figure on the top right shows the entire assembly prior to lowering in the dewar. Orange cable delivers laser or LED light that shines on the SiPMs. Everything is secured to the wooden lid that closes the dewar.

`fig:sipm_mount`

2 pins is used (based on the previous design by the CSU group) to provide contact to
 3 SiPMs and hold them in place with acrylic housing rather than solder joints. Special
 4 cryo-rated, compact MMCX connectors have been acquired, as the solder joints of
 5 the signal and power wires have been breaking from repeated usage.

6 The SiPM bias voltage is delivered via the POGO pins and the SiPM signal is sent
 7 via these pins to the DAQ. The signal is amplified via two inline low-noise amplifiers
 8 and read out by oscilloscope. SiPMs are illuminated by 1-ns-long laser pulses from
 9 the tunable wavelength laser system. Laser light intensity is regulated with a Fine
 10 Laser Intensity Controller (FLIC), a computer-controlled system that allows tuning
 11 of laser intensity through several orders of magnitude with various stages; this is
 12 important for linearity measurements. Signal waveforms from a Waverunner LeCroy
 13 oscilloscope are recorded and analyzed.

14 It has also been noted that the SiPMs require lower bias voltage when cooled
 15 in LN₂, which requires determination of the optimal operating voltage at LAr tem-
 16 perature, since dark rates also increase with bias voltage. Additional tests showed
 17 excellent gain at cryogenic temperatures, as can be seen from the tests conducted
 18 on the SenSL C series SiPM MicroFC-600-35-SMT (previous M and B series also
 19 tested)

do we need prev (...)?

20 shown in Figure ??, along with clearly distinguished pulses for one, two, three
 21 and four photoelectron pulses.

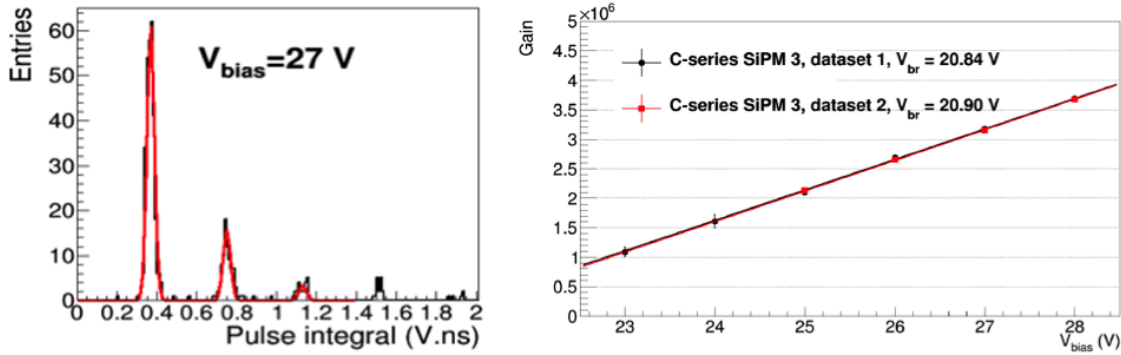


Figure 1.10: SiPM SenSL C series gain tested in LN2 is shown on the right hand side. Excellent linearity over the entire overvoltage range observed. There is a significant change of gain with increasing bias voltage, effectively doubling between the minimum and maximum tested bias voltage. Clearly distinguished numbers of photoelectrons can be seen in the left hand figure.

fig:sipm_gain

2 The dark rate increases significantly with bias voltage, but the overall rate is very
 3 small when SiPMs are cooled to 80 K, as can be seen in Figure ??.

4 Afterpulsing is another important aspect of SiPM performance. Afterpulsing
 5 increases noise and obstructs detection of late argon scintillation light. Results of
 6 the afterpulsing measurement performed on the cooled SenSL C series SiPM show
 7 a very small afterpulsing fraction below 1% for most overvoltage values, as can be
 8 seen in Figure ??.

9 SenSL C series SiPMs were also tested for cross-talk. Cross-talk gives a measure
 10 of the light hitting one pixel

this seems wrong, plz check

11 , also produces signal in adjacent pixels and effectively distorts the signal strength.
 12 Figure 1.13 shows the test results. Cross-talk is a strong function of overvoltage,
 13 which will be another criterion in choosing the operating overvoltage for the PD
 14 system.

15 Although not presented here, SenSL B series SiPM MicroFB-600-35-SMT were
 16 also tested and satisfy our requirements, based on the tests conducted so far. How-

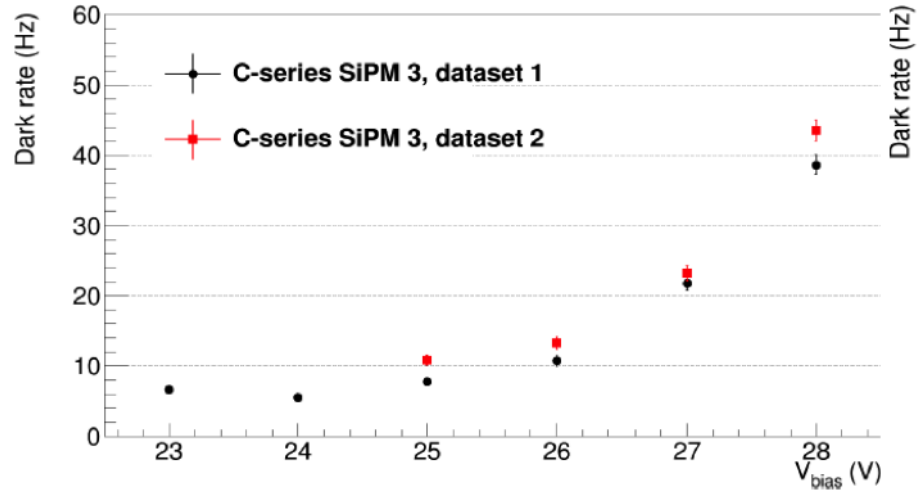


Figure 1.11: SiPM SenSL C series dark rate with two different data runs in LN2. While dark rate increases for an order of magnitude, it is still less than 50 Hz even at the highest bias voltage setting.

fig:sipm_dark

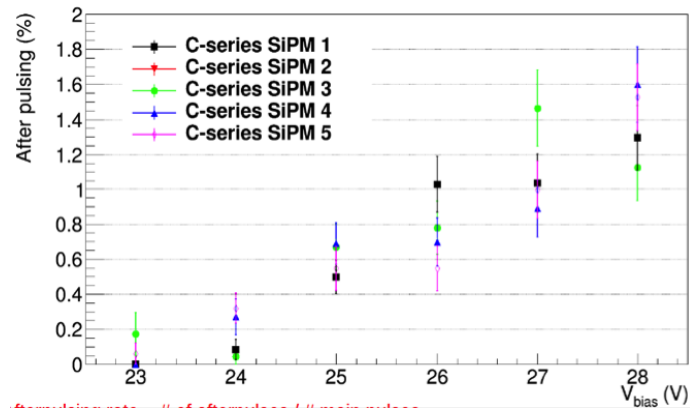


Figure 1.12: SenSL C series SiPM afterpulsing fraction for 5 different SiPMs, with system being completely cooled down.

fig:sipm_after

ever, we have not performed yet a full set of tests including mechanical integrity from thermal cycling and cross-checks.

Is this in the running? If not, leave out. If so, why not mentioned till now?

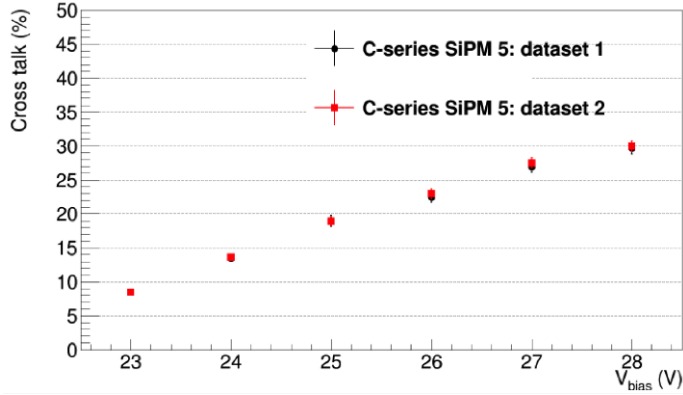


Figure 1.13: SenSL C series SiPM cross-talk measurement based on two separate runs in LN₂. Cross-talk is a strong function of overvoltage and is very consistent between the runs.

fig:sipm_cross

In parallel with performance tests, mechanical cryogenic tests are being conducted where the number of cycles and time spent at LN₂ temperature is being logged. This important test has started recently, but will involve testing a number of devices for extended period of time and examining their mechanical status under the microscope.

Future steps involve increasing the testing sample of C series SiPMs and evaluating several alternatives to avoid the risk of sole-source vendor.

1.5 Mechanical Support

Mechanically supporting the PD systems in the APA frames presents several challenges, including the need to support three different light-collecting and wavelength-shifting technologies in a package utilizing the same mounting features in the APA frames, and the effects of varying thermal contraction of various materials at 80 degrees Kelvin which complicated both light collector and SiPM mounting.

devices of the 3 technologies are packaged together and the package is mounted on the apa? or the three all use the same mounting features? I'm confused

The baseline
reference?

36 design for mounting the PDs into the APA frames calls for ten PD modules,
37 approximately 2.2 m long, mounted with roughly equal spacing along the full length
1 of the APA frame (Figure 1.14). The PD modules are read out using individual
2 twisted-pair cable, one per SiPM. These cables (120 of them in the original baseline
3 reference?

4 design) are routed through the APA side tubes to a connector at the cold elec-
5 tronics readout end of the APA. Initially it was decided that it would be too com-
6 plicated to design the APA frames to allow PD module installation following APA
7 wire-wrapping, so it was planned to install the PD modules prior to this step. The
8 wavelength-shifting elements in the light collectors of the PD modules are sensi-
9 tive to heat, humidity and most critically to ambient light, which places significant
10 requirements

11 constraints?

12 on the environment in which the APAs are assembled and stored,

13 Something about how this is still better than installing them after wire-
wrapping; list a risk or two of that method, maybe, for comparison

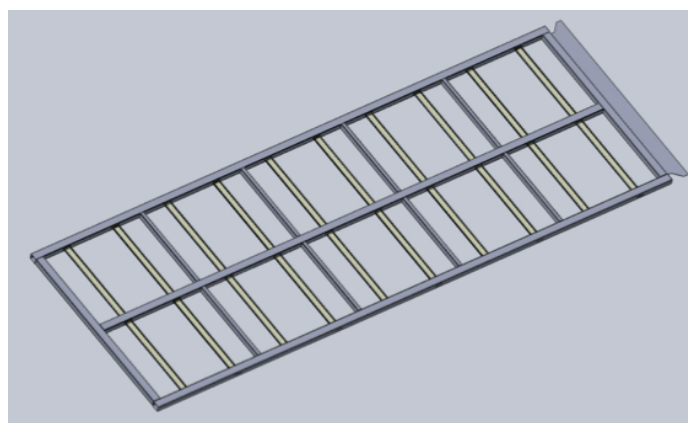


Figure 1.14: Full APA frame with ten photon detectors mounted inside the frame

fig:5.5-1

14 A universal PD frame assembly was devised to hold all three PD design variations
15 under consideration. Figure 1.15 shows an example of a short (400-mm-long active
16 area) version of this frame manufactured for the 35t test,

17 figure could use labeling

18 and Figure 1.16 shows a mechanical assembly drawing of the frame system for one
19 of the candidate light collector choices. The frame consists of two plastic (acetal) end

20 caps mounted to the inside of the APA frame, joined by 10-mm-diameter stainless
21 steel tubes that run the full width of the APA frame, providing intermediate support
22 for the PD modules. The SiPM mount PCBs

I can't parse this phrase

23 are incorporated into one of the end blocks, along with the cable connections
24 for the twisted-pair cables. Due to the significant difference between the coefficients
25 of thermal expansion for the stainless steel frame and the plastic WLS elements, a
26 relative difference in thermal contraction of $\sim 1\%$ is expected at LAr temperatures.
27 The far endblock assembly provides balancing forces to the light collector elements
28 to ensure these elements remain straight and in good contact with the SiPMs.

29 Testing of the PD mount scheme in many test setups (at IU, CSU and FNAL),
30 as well as experience APA assembly, have led to a re-evaluation of the PD mounting
31 scheme. The revised baseline

32 has PD installation after ^{Fig. 5.5-4}APA wire wrapping, through slots left in the side of
33 the APA frame (Figure 1.17). As shown in the figure, the plan still calls for ten
34 PDs per APA frame. Five of the PDs will be installed through each side of the
35 APA frame, and the cables for each of the PDs will be routed to the cold-electronics
36 end of the APA, inside the side tube through which the PD was inserted. Stainless
37 steel c-channels mounted into the APA frames prior to wire wrapping will guide and
38 support the PDs during and after installation. The PD will only be attached to
39 the APA frame at one end, so the purely plastic PD module ^{Fig. 5.5-5}will be free to slide in
40 the track to allow for the differential contraction (Figure 1.18). Tests of the 2.2-m
41 prototype assemblies of both fiber hybrid and the LSU-proposed monolithic acrylic
42 bar design in the CSU CDDF

43 what's cddf?

44 have demonstrated significant promise.

45 Thermal contraction at cryogenic temperatures also complicates the mounting of
46 the SiPMs in the PD modules. The baseline

47 sensL SiPMs are surface-mount components, with four 0.5×0.5 -mm pads for
48 making electrical contact. Unreliability

49 ?

50 and elevated dark count rate problems, as well as physical delamination of the
51 SiPM front face from the silicone substrate, were observed early in cryogenic testing
52 of SiPMs, and suspicion fell on the mechanical contact between the mounting PCB
53 and the SiPM itself.

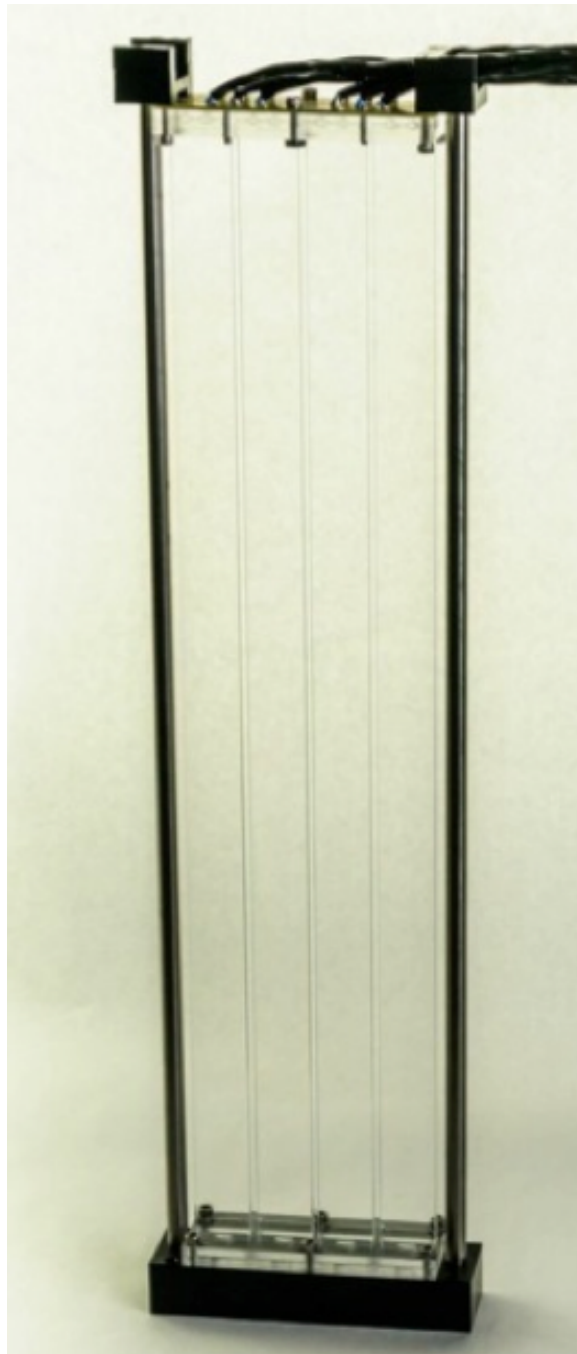


Figure 1.15: Photograph of 40 cm long bar-based prototype mounted in test frame

fig:5.5-2

Design for a Deep Underground Single-Phase LArTPC

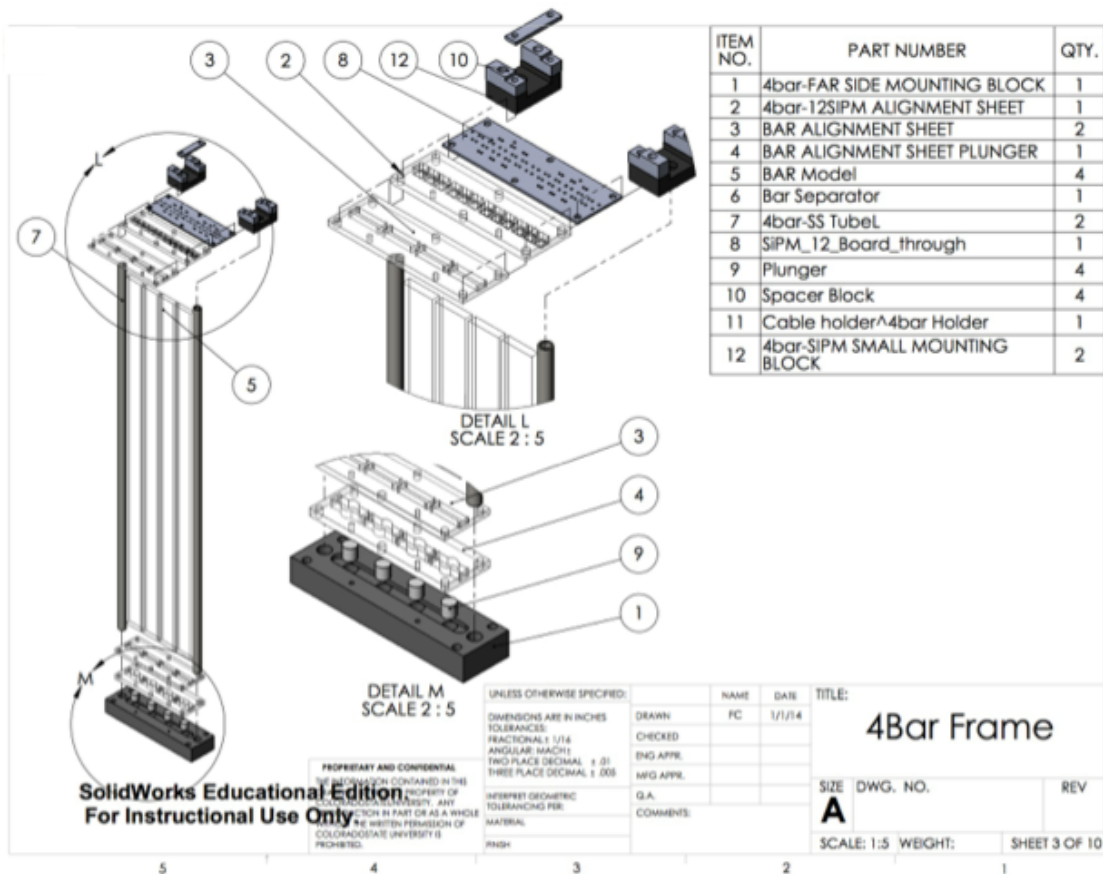


Figure 1.16: Mechanical assembly drawing of frame system

fig:5.5-3

Design for a Deep Underground Single-Phase LArTPC

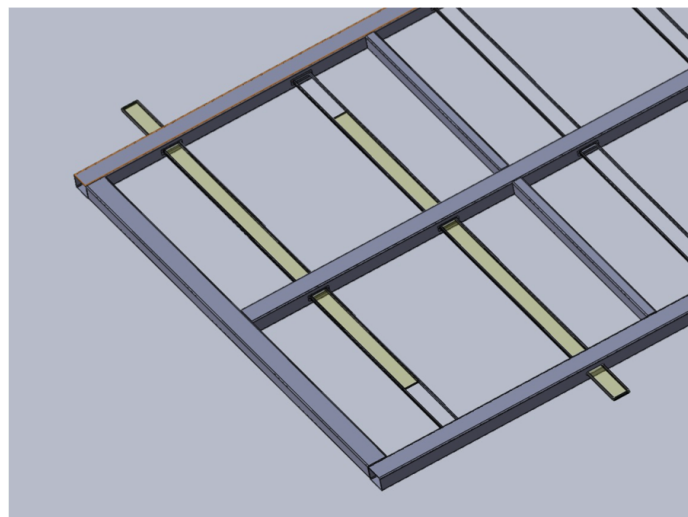


Figure 1.17: Blow up of APA fram showing PD insertion location

fig:5.5-4

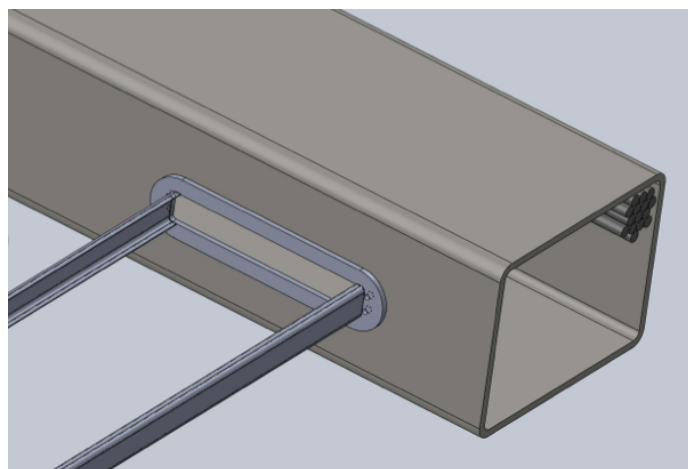


Figure 1.18: Slot and rail showing mounting location of photon detector

fig:5.5-5

8 Three different methods of making these electrical contacts have been tested

9 ?

10 :

11 • Soldering the SiPMs directly to the PCBs (fig 5.5-6a),

12 • using commercial spring-loaded electrical contacts or “Pogo pins” (Figure [fig:5.5-6b](#)??),

13 [check ref](#)

14 • soldering short wires to the SiPM pads and thence to the PCB (Figure [fig:5.5-6c](#)??).

15 [check ref](#)

16 Each of these methods provides assembly challenges, and cryogenic testing has not
17 suggested a clear choice so far. Testing and development are still underway to resolve
18 this issue.

19 **1.6 Photon System Readout Electronics**

sec_elec

20 **1.6.1 Reference Design**

21 Scintillation light from LAr comes from the two different excited states

22 of Ar atoms?

23 with lifetimes of about 6 ns and 1.6 μ s. Only a limited amount of light

24 can you be a bit more specific?

25 is collected by the PD system, so the electronics must be designed to collect
26 the light from both excited states. A summary of the general requirements for the
27 system, including requirements from a physics performance perspective, are given in
28 Table [tab:ref](#) 1.3.

29 The plans for the electronics for the photon detection subsystem include a baseline

30

31 design with several options that remain R&D activities. There alternative implementations of electronics are described in Section 1.6.2.

32 In the baseline

33

34 plan, there are no front-end electronics in the cold volume. Instead, the unamplified signals from the SiPMs are transmitted to outside the cryostat on cables for

Table 1.3: Physics requirements for the photon detector electronics

| Performance Parameter | Target |
|-----------------------|--|
| Time Resolution | Better than 30 nS wrt event time zero ("t0") |
| Charge Resolution | 0.25% photo-electron equivalent |
| Dynamic Range | $\sim \times 10$ better than detector (1000:1) |
| Linearity | Sufficient to resolve 1 photo-electron signals |
| Multi-Hit Capability | Sufficient to measure Triplet (late) Photons |
| Dead Time | Live up to 2 drift times either side of beam spill |
| Bias Control | 0.1 V resolution up to 30 V per channel |
| Calibration | On-board Charge Injection |
| Timing | Events time-stamped using NO ν A Timing syst. |

tab:fee_req

5 processing and digitization, as shown in Figure 1.19. There are advantages and dis-
 6 advantages to this approach. The advantages are that the infrastructure required
 7 for inside the cryostat is reduced (power, data cables, precision clocks, data proto-
 8 cols, etc.); reliability is improved (no single-point failures of multi-channel devices
 9 inside the cryostat); serviceability and accessibility to the front-end electronics are
 10 improved; and the need to develop cold electronics, possibly a custom ASIC, is elim-
 11 inated. The disadvantages are that the cable plant inside the detector is increased,
 12 which can create mechanical challenges and installation difficulties; the flange board
 13 (warm/cold interface) is more complex; there are generally more connectors in the
 14 system; and signal-to-noise considerations are more difficult. The baseline

15

16 design favors simplicity, reliability and reduced R&D time and costs, and also
 17 meets the performance requirements of the electronics.

18

No fig1 exists for: Block diagram of the photon detector signal processing sys-
 tem.

Figure 1.19: Block diagram of the photon detector signal processing system

fig:fig-e-1

19 In the 35t prototype, each SiPM signal was
 20 not ‘is’?

21 transmitted on an individual shielded twisted-pair cable fitted with individual
 22 LEMO-style connectors. The bias voltage was coupled onto the signal cable, using
 23 AC-coupling on the receiving end to measure the SiPM signal. The use of high-

24 quality cable with point-to-point connections between an individual SiPM inside the
25 cryostat and the front-end electronics residing outside the cryostat, combined with
26 good differential signal processing on the receiving end, enabled the demonstration of
27 the principle that single photo-electron signals could be measured accurately without
28 the need for cold electronics. In order to address the problems with the cable plant
29 as identified above, the following ideas are being pursued:

- 30 • Ganging together several SiPM outputs from a given PD detector into one
31 output cable. This increases the detector capacitance, affects the pulse shape,
32 and could spoil the timing resolution of the measurement. Also, the SiPMs
33 may have to be preselected, since there will be only one bias voltage for three
34 devices, and it may be important to match the overvoltage characteristics.
35 Studies are in progress to find a compromise between data precision and cabling
36 issues. One approach is to add a cold pre-amplifier if the ganging together of
37 several SiPMs result in performance that is too degraded to meet specifications.
38 The infrastructure requirements (cables, connectors, power, cold performance,
1 reliability, mechanical mounting, etc.) would have to be considered.

- 2 • Use of multi-conductor, individually shielded pair

3 if it's a pair, is it just dual-conductor? This is confusing

4 cable. A candidate cable containing four individually shielded twisted pairs has
5 been identified and tests are in progress. The cable is in Teflon jacket, which
6 should be

7 has been found to be?

8 acceptable for use in LAr.

- 9 • Use of mass-terminated connectors. Several candidate connectors for use with
10 the cable described above are being pursued.

11 The baseline

12 plan assumes that three SiPM signals
13 outputs?

14 can be ganged together into one readout channel. By using the multi-conductor
15 cable with four twisted pairs, this results in one cable per PD consisting of 12 SiPMs.
16 The diameter of this cable is xxx-mm,

17 get number

which reduces the cable plant by $\sim \times 10$ compared to that used in the 35t detector.
The cost of the connectors also decreases by $\sim \times 10$. Lastly, the ease in making
connections at the flange board will be improved by the use of a mass-terminated
connector.

In the baseline

plan, the front-end electronics reside outside of the cryostat in instrumentation
racks. A custom module for receiving SiPM signals has been designed and built, and
signal processing is being performed in the front-end as preprocessing for trigger and
DAQ. The module is called the SiPM Signal Processor (SSP). An SSP consists of 12
readout channels packaged in a self-contained 1U module. Each channel contains a
fully differential voltage amplifier and a 14-bit, 150 MSPS analog-to-digital converter
(ADC) that digitizes the waveforms received from the SiPMs. The front-end amplifier
is configured as fully differential with high common-mode rejection, and receives the
SiPM signals into a termination resistor that matches the characteristic impedance of
the signal cable. Currently there is no shaping of the signal, since the SiPM response
is slow enough relative to the speed of the digitization to obtain several digitized
samples of the leading edge of the pulse for the determination of signal timing.

The digitized data is stored in pipelines in the SSP for up to $\sim 13 \mu\text{s}$. The
processing is pipelined, and performed by a Xilinx Artix-7 Field-Programmable Gate
Array (FPGA). The FPGA implements an independent Data Processor (DP) for
each channel. The processing incorporates a leading-edge discriminator for detecting
events and a constant fraction discriminator (CFD) for sub-clock timing resolution.
Because the FPGA is programmable and accessible, it is possible to explore different
data processing algorithms and techniques, and even customize the readout for a
given type of event (e.g., supernova). A picture of the module is shown in Figure 1.20.
Fig:fig-e-2
A block diagram of the system is shown in Figure 1.21.
Fig:fig-e-3

In the simplest mode of operation, the module can perform waveform capture,
using either an internal trigger or an external trigger. Up to 2046 waveform samples
may be read out for each event. When waveform readouts overlap, the device can
be configured to offset, truncate or completely suppress the overlapping waveform.
Pile-up events can also be suppressed.

As an alternative to reading full waveforms, the DP can be configured to perform
a wide variety of data processing algorithms, e.g., measuring amplitude (via several
techniques), and timing the event with respect to a reference clock. All timing and
amplitude values are reported in a compact event record. Each data processing
channel stores up to 340 event records when not storing waveforms.

Generally,

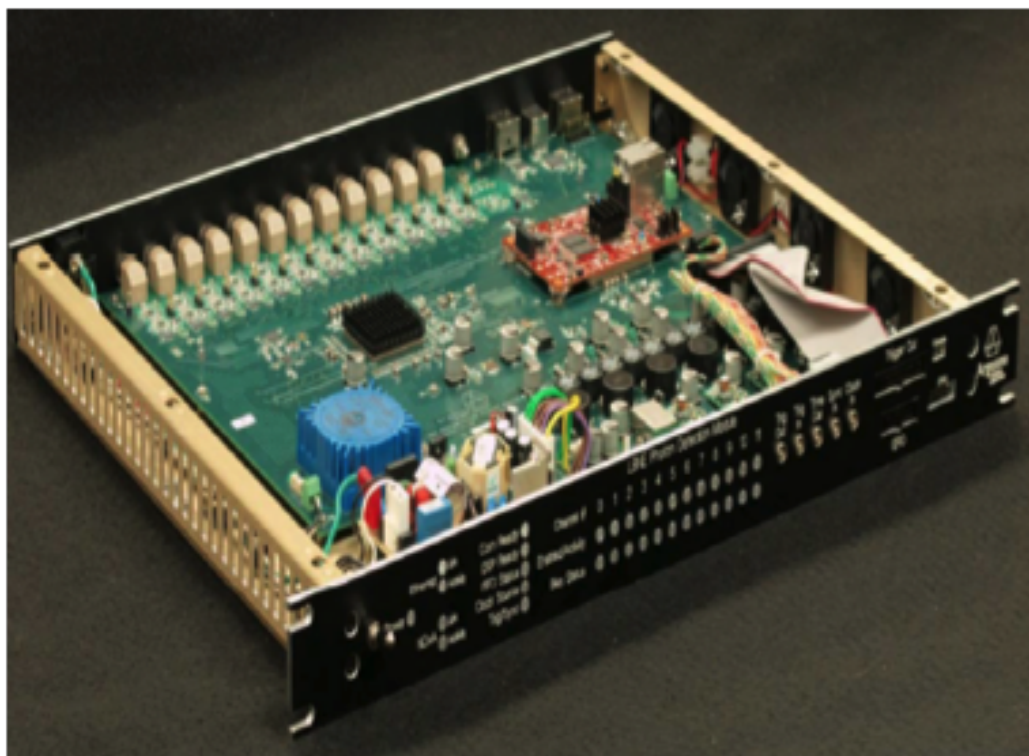


Figure 1.20: Picture of the SSP module

fig:fig-e-2

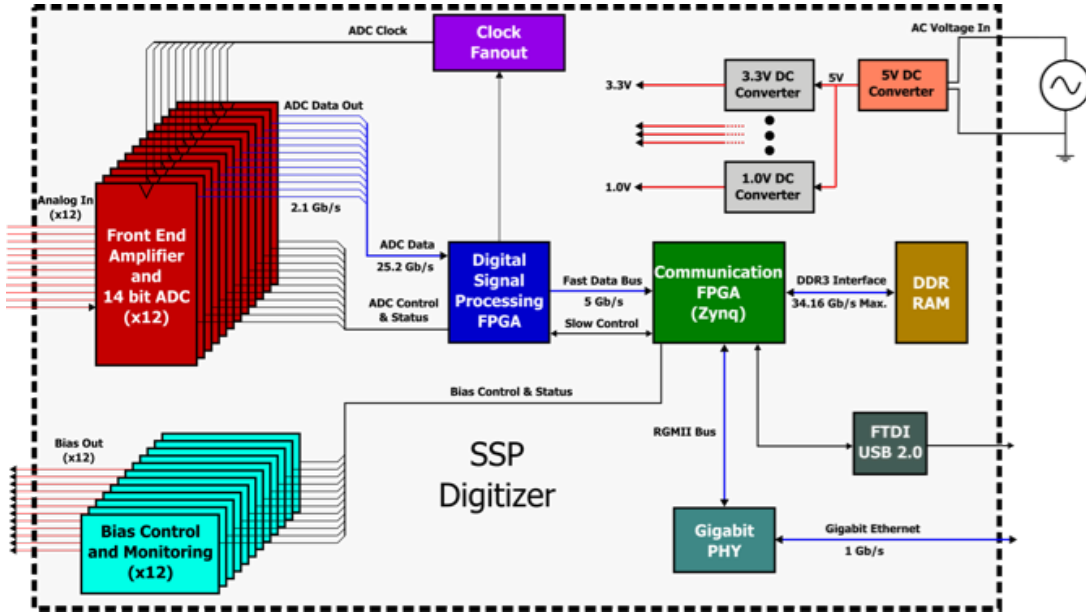


Figure 1.21: Block diagram the SSP module

fig:fig-e-3

There's that 'generally' again!

the SSP performs pipelined processing. The module has been designed to support several different triggering schemes, including self-triggering, use of an external trigger, or use of an external gate to read out all events within a time window. In order for the events measured in the photon detector to be matched up with the corresponding events in the TPC, the front-end electronics attaches a timestamp to the data as it is acquired. The timestamp is unique, and has a correspondence with the timestamps in the TPC electronics processing. The timestamp in the SSP is applied to the event data as it is digitized, and becomes part of the data as the processing proceeds. In the case where zero-suppression and data sparsification are used, the timestamp on accepted data remains intact. To achieve this, the TPC and PD electronics must be synchronized, including timestamp counter resets, and a known and stable calibration between the corresponding timing resolution of the ADC conversion in the two systems

not full sentence

. The electronics has been designed to support a full interface to the NO_νA timing system, which is the baseline

27 timing system for the experimental prototypes.

28 A Xilinx Zynq FPGA, onboard a MicroZed system-on-module,

29 ‘the’ makes it sound like we’ve heard of the microzed thing, but we haven’t yet

30 handles the slow control and event data transfer. The SSP has two parallel
31 communication interfaces, USB 2.0 and 10/100/1000 Ethernet. The 1-Gb/s Ethernet
32 supports full TCP/IP protocol. The module includes a separate 12-bit high-voltage
33 DAC for each channel to provide up to 30 V of bias to each SiPM. The module also
34 features charge injection for performing diagnostics and linearity monitoring, and
35 also voltage monitoring.

“The module also features charge injection for performing diagnostics, linearity
monitoring and voltage monitoring. ” or “The module also features charge in-
jection for performing diagnostics and linearity monitoring, and it also features
voltage monitoring. ”?

36 In tests to date, the SSP is capable of measuring single photo-electron signals
1 coming from the SiPMs over a cable length of 30 m when the SiPMs are operated
2 at LAr temperature. The timing resolution of the signals has been measured to be
3 better than 3 ns. The full-differential signal processing in the front-end circuitry is
4 important in achieving this result.

5 The SSP is self-contained in that it receives 60-Hz, 120-V power, and has internal
6 linear and DC/DC power supplies for generating the DC voltages needed for the
7 instrumentation and the bias voltage for the SiPMs. The SSP is packaged in a 1U,
8 rack-mountable package. For the 35t prototype, the racks are located near the ports
9 on the top of the cryostat.

11 1.6.2 Alternatives

sec_alt 12 Start with a sentence that says what alternatives this section discusses: CE,
pulse-shaping, ASIC...

13 In the baseline

14 15 design of the PD electronics, no electronics are placed inside of the cold volume.
16 This results in a large number of cables and connectors. Other experiments using liq-
17 uid argon have successfully implemented cold TPC electronics, thereby significantly
18 reducing the cable plant that must come through the cryostat.

19 Using cold electronics

20 check

21 has challenges in power distribution, heat dissipation, and the performance of
22 front-end electronics in LAr. To address serviceability, the cold electronics might
23 be realized in a modular way and situated just below the flange in the cryostat so
24 that it can be accessed for repair if needed. To this end the zero suppression will
25 be important to avoid high data rates depending on the number of readout channels
26 needed.

27 prev sentence unclear. what depends on no. of channels?

28 The cold zero suppression could be implemented by means of a cold FPGA (or
29 an ASIC, yet to be developed). To date the cold FPGAs have had mixed results in
30 tests.

31 Performing an “analog zero suppression” with a constant-fraction discriminator
32 provides an alternative approach; it would be followed by gating the signal and
33 performing warm digitization. This technique would, however, introduce the com-
1 plication of encoding the particular channel.

I'm not sure I got this right; I didn't completely understand the orig sentence to
begin with

3 The significant challenges in this technique include power dissipation, the in-
4 creased possibility of contamination of the LAr, and extended infrastructure that
5 must reside in the cold volume. On the other hand, it can significantly reduce the
6 number of signal penetrations into the cold volume.

7 The electronics for the photon detector of LBNE uses fast (direct) digitization of
8 the SiPM pulses. Another option for the front-end electronics is to use pulse shaping.
9 Instead of digitizing the full bandwidth of the SiPM signal, in this technique the
10 pulse is shaped using analog filtering techniques, generally producing a pulse with a
11 prescribed shape for which the peak is proportional to the total amount of charge.
12 By measuring the peak, both amplitude and pulse timing can be obtained. Since
13 the pulse response follows a known transfer function, the pulse peak can be obtained
14 using slower synchronous sampling, or using asynchronous sampling through the use
15 of peak detection and constant fraction discrimination.

16 In either case, the data can be processed by an FPGA using algorithms optimized
17 for the application. In particular, assuming that a sufficient number of samples of
18 the shaped pulse are obtained, a chi-square comparison of the shape to the ideal
19 pulse shape can be used to identify events or determine pulse corruption

check

21 and a timestamp can be synchronized using an external clock source. The data
22 can be read out in a similar manner, using USB 2.0 or 10/100/1000 Ethernet. The
23 virtue of this approach is that a slower ADC can be used, reducing power consump-

24 tion, data load and the speed of readout links.

25 reducing speed of readout links is a virtue?

26 The technique trades bandwidth for shaping, making timing and pile-up issues
27 more important. This can result in making the interpretation of the pulse shape
28 more complex, requiring more than direct digitization. Generally, the pulse-shaping
29 circuitry is also less expensive than the direct digitization technique, assuming similar
30 performance requirements.

31 Another option for the photon system readout would include the use of an Application
32 Specific Integrated circuit (ASIC) as a way to reduce cost. The large channel
33 count in a real detector system is such that the production cost of the system could
34 be greatly reduced.

35 how does large channel count relate to reduction in cost?

36 Often, the cost of development of an ASIC from scratch is quite high, of order
37 ~400K\$, and can take ~1 to 2 years for development, so cost and schedule must
1 be weighed carefully. However, other benefits from the ASIC approach include re-
2 duced space requirements for circuitry on the front-end, lower power dissipation, and
3 specialized functionality in the front-end chip.

4 Several ASICs have been designed over the last few years for SiPM readout. It
5 would be possible to explore the functionality and performance of these designs, for
6 either for warm or cold electronics, and evaluate their suitability for LBNE. Direct
7 digitization has the virtue of being straight-forward from a circuit design perspective.

8 connect direct digitization with ASIC

9 By taking advantage of modern high-bandwidth OP amps, high-speed, high-rate
10 ADCs, and powerful FPGAs with high-speed serial links, it is possible to obtain 14-
11 bit dynamic range digitization with ~1-ns timing resolution. By reading all of the
12 samples into an FPGA having a deep buffer, digital signal processing techniques can
13 be employed using the programmable logic; this could make it possible to develop
14 powerful analysis algorithms in time. The technique generally has higher power con-
15 sumption and tends to be more expensive than simpler instrumentation techniques.

16 1.7 Photon Detector Calibration

17 sec_pd_calib The photon detector calibration is a part of a larger calibration plan that covers
18 all aspects of a LArTPC detector calibration. The larger plan includes methods to
19 convert collected charge to initial particle energy, as well as calibration techniques to

20 convert collected scintillation light into an estimate of a particle's interaction time,
21 energy and a track/vertex location for each event.

22 As already described, the baseline

23
24 for the scintillation photon detectors assumes employment of acrylic light col-
25 lection paddles to reduce the required costly photo-cathode area. Several photon
26 detector designs are presently being developed and are being tested in small dewars.
27 Since none of these new elements has yet been tested in a large-scale TPC, the 35t
28 LArTPC prototype is being constructed to provide essential design validation.

29 The current FD designs are anticipated to have sufficient sensitivity to provide
30 event timing information for atmospheric neutrino and proton decay channels. How-
31 ever, it will not provide high efficiency down to the 5-MeV neutrino energy level
32 desired by the supernova program. This would cause the supernova event recon-
33 struction energy resolution to be 20% compared to the 5% achievable with a photon
34 detector able to operate efficiently at a sufficiently low energy threshold. The im-
35 provement in physics will be studied in the near future but a substantial effort in
1 development of improved detection techniques is desired.

2 In the absence of precise physics requirements for the photon detector system
3 and in order to support R&D activities on the photon detector development it was
4 decided that the photon detector should provide a time stamp to determine the time
5 of occurrence of an event (so called "time zero") with an accuracy much better than
6 1 s

7 fix

8 .

9 Items relevant to the photon detector calibration are the fast and slow components
10 of the light, photon propagation including scattering and reflections, impact of N2,
11 what's N2?

12 E-field strength, and the energy range of interest. A calibration system that
1 addresses the issues listed above has to be both comprehensive and cost-effective,
2 and has to be tied to the overall calibration system that includes both charge and
3 scintillation-light calibration techniques. Such a system will be designed in the future.

4

5 'is planned...?'

6 To support the PD R&D phase a light-flasher-based calibration system has been
7 designed that will serve to monitor the relative performance and time resolution
8 of the system. In particular, for the anticipated 35t performance tests the relative
9 efficiencies of multiple light collection techniques must be evaluated in order to down-

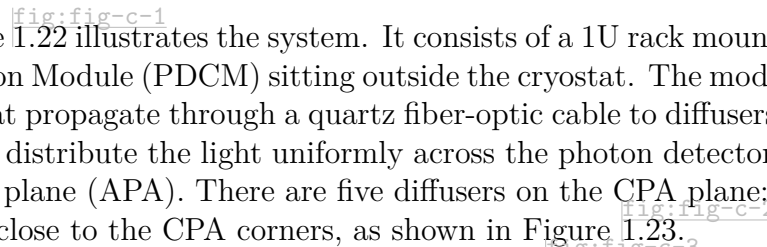
10 select an optimal light-readout technology. The system that meets these requirements
11 will consist of a set of LEDs as light sources or a laser with a VUV wavelength coupled
12 to quartz fibers, thus transmitting light from outside the detector volume to desired
13 locations at the CPA within a TPC. Therefore the 35t detector will be equipped with
14 LEDs located and fired externally, with fibers running into the cryostat to diffusers
15 that will emit light from the CPA to the APA.

16 For the 35t cryostat, installed at the surface at Fermilab, a light-flasher-based
17 calibration system will be complementary to calibration by cosmic-ray muon tracks.

18 The
19 **35t calibration?**

20 measurements should be performed with an UV (245-375nm) light source. The
21 UV light mimics physics starting from the wavelength shifter conversion, through
22 the light guide propagation, photo-sensor detection and FEE readout. The external
23 light-flasher calibration system is designed such that it:

- 24 • is simple to implement (has no active components within PD/APA, such as
1 LEDs or fibers mounted within APA).
- 2 • is less-intrusive (less fiber material is within detector than if each PD frame
3 were equipped with individual fiber).
- 4 • provides a benchmark light-based reconstruction with the use of localized light
5 sources distributed throughout the detector volume.
- 6 • has the potential to be adapted for deployment in a large far detector

7 
Figure 1.22 illustrates the system. It consists of a 1U rack mount Photon Detector
8 Calibration Module (PDCM) sitting outside the cryostat. The module generates light
9 pulses that propagate through a quartz fiber-optic cable to diffusers at cathode-plane
10 (CPA) to distribute the light uniformly across the photon detectors mounted within
11 an anode plane (APA). There are five diffusers on the CPA plane; one in the center
12 and four close to the CPA corners, as shown in Figure 1.23.

13 The PDCM module layout is shown in Figure 1.24. The ANL photon calibration
14 module is based on a repurposed SSP unit. An SSP board will be repackaged into a
15 deeper rack mount chassis that will accommodate a new internal LED Pulser Module
16 (LPM) and an additional bulk power supply. The LPM utilizes five digital outputs
17 to control the LPM pulse and its duration (arrows in black). These LVDS outputs
18 are derived from the charge injection control logic within the SSP's FPGA. The
19 even-channel SiPM bias DACs are repurposed to control the LPM pulse amplitude
20 (arrows in red). The adjacent odd channels are used to read out a photodiode that

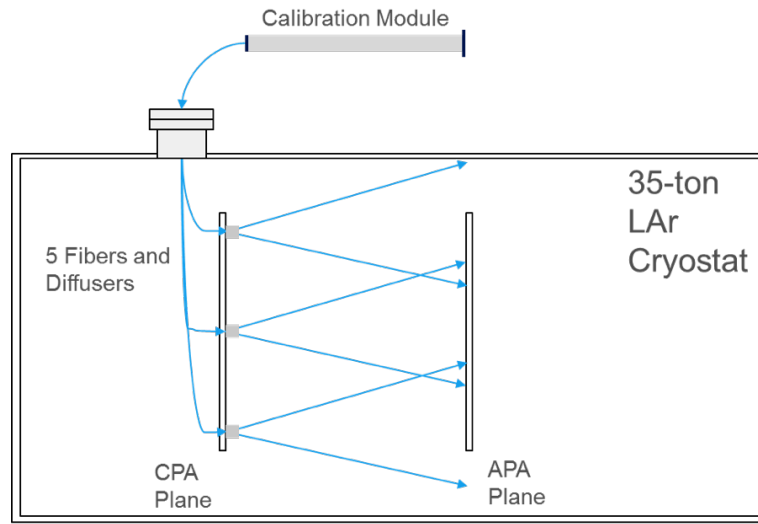


Figure 1.22: Concept of the UV-light calibration system for the photon detector in liquid argon

fig:fig-c-1

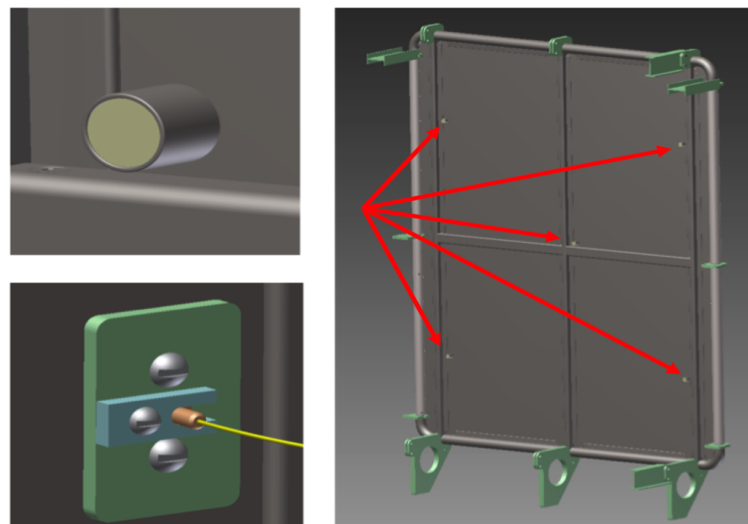


Figure 1.23: The diffuse light is emitted from diffusers (top left figure) mounted at five CPA locations, indicated by arrows (right figure). The UV light from the PDCM to diffusers is transported through quartz fiber (lower left figure).

fig:fig-c-2

21 is used for pulse-by-pulse monitoring of the LED light output. The output of the
 22 monitoring diode is used to normalize the response of the SiPMs in the detector to
 23 the calibration pulse

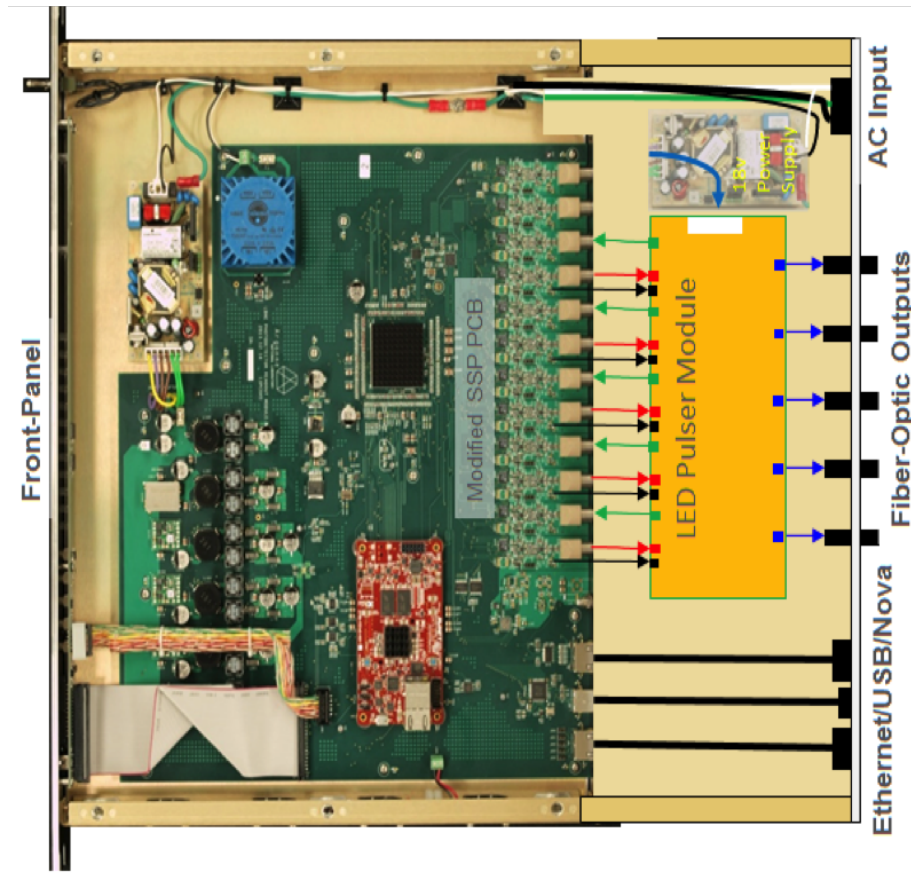


Figure 1.24: Photon detector calibration module (PDCM) layout

`fig:fig-c-3`

24 The designed diffuse-light calibration system has been performed with 280-nm
 25 light using TracePro, a generalized 3D light ray-tracing program with the ability to
 26 include bulk optical properties such as absorption, fluorescence and birefringence in
 27 addition to surface properties such as scattering and reflection. Figure 1.25 shows
 28 simulated light distributions of the 35t APA for the cases of the VUV light emitted
 29 by either the central diffuser only (left figure), or by the outer four diffusers simulta-
 30 neously (right figure). A full Geant4-based simulation of the detector will be used
 31 in the future. Using the preliminary data with the 35t-style light guides (indicating
 32 0.5% efficiency for number of photo-electrons per incident 128-nm LAr scintillation

33 photon 50 cm from the light guide), we estimate for 280-nm light to observe \sim 15
 1 photo-electrons per single SiPM channel when the light is emitted from the single
 2 central diffuser in 13-ns-long pulses. Similarly, we expect \sim 100 photo-electrons ob-
 3 served by a single SiPM channel when 280-nm light is emitted in 100-ns-long pulses
 4 from the four outer diffusers at once.

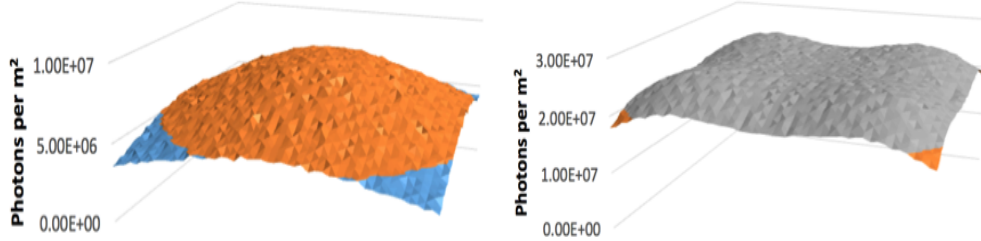


Figure 1.25: Simulated light distributions of the 35t APA for the cases of the VUV light emitted by either the central diffuser only (left), or by outer four diffusers simultaneously (right).

fig:fig-c-4

5 In the LBNE prototypes (i.e., the 35t) and in the far detector it will be important
 6 to check that photon-detector components are functioning properly at various stages
 7 of the detector operation. Periodic light-source deployments will monitor the sys-
 8 tem's stability as a function of time. A change in the relative difference of UV light
 9 responses will point towards potential wavelength-shifter instability, changes in SiPM
 10 gain and collection efficiencies. It is expected that much of the same monitoring can
 11 be done with cosmic rays in the 35t (at the surface) using periodic LED/laser calibra-
 12 tion runs complemented with cosmic-ray data tracked with an external hodoscope.

13

14 **that's a mouthful**

15 With the 35t detector one could use a well-defined muon trajectory defined by
 16 the hodoscope geometry and monitor the number of p.e.'s per MeV of deposited
 17 charge. The number of p.e.'s per PD channel from the muon track could be used as
 18 a calibration constant. However, for the deep underground detector the cosmic-ray
 19 flux may be inadequate for timely monitoring of the photon detectors. Two sets of
 20 calibration runs are planned for the 35t detector:

- 21 1. Calibration runs with four outer diffusers running simultaneously, in order to
 22 -measure response of PD channels in multi-p.e. range and get integrated
 23 number-of-event samples for each channel (for maximum light output)

- 24 -test the dynamic range from 1 p.e. to maximum number of p.e.'s.
25 -repeat runs periodically to track any changes in channel response.
- 26 2. Runs with central diffuser only, in order to perform
27 -initial calibration runs that will reveal malfunctioning channels, if any
1053 -timing measurements with the 10–50-ns pulses to verify time resolution of the
1054 PD system.

1055 The controlled source of light described here will be used to perform a relative t_0
1056 calibration, where the t_0 could be absolutely calibrated with the use of the cosmicray
1057 triggers available with 35t detector. Effects that contribute to a finite time resolu-
1058 tion and relative time offset of PD channels include: scintillation time constants,
1059 photon conversion with wavelength shifter, photon propagation through PD paddle,
1060 SiPM jitte, and FEE resolution. Most of these effects are constant and can be in-
1061 dividually measured on the bench, so the LED flasher system will monitor overall
1062 stability of the photon detector. To go beyond the current R&D phase one needs
1063 detailed MC simulations of light production, propagation and detection. This will
1064 allow comparisons of reconstruction performance against prototype data in terms of
1065 calorimetric energy and position reconstructions for measured event tracks. Future
1066 light-collection systems will aim to maximize the active area of the light guide bars,
1067 to achieve a high photon-detection efficiency with an optimized timing and granu-
1068 larity required for improved position resolution. As in the case with the TPC charge
1069 calibration we will need to evaluate what may be achieved with expected cosmic-ray
1070 muons and Michels, π^0 , and natural radioactivity events (such as ^{39}Ar with end-point
1071 energy of about 500 keV).

1072 1.8 Installation

1073 Installation of the photon detectors is one of the most significant factors driving the
1074 mechanical design. As discussed above,

1075 give section

1076 the initial thought was to install the PDs and run the SiPM twisted-pair cable
1077 down the frame side tube prior to wire-wrapping the APA. After experience with the
1078 environmental controls (primarily UV filtered light) required by the PDs, as well as
1079 the difficulties in dealing with the PD readout cable ends during wire-wrapping, it
1080 was decided to change the baseline

such that the PDs would be inserted after wire wrapping is complete. In addition to relaxing the physical constraints on the wire wrapping, this also relaxes a schedule connection between the APA and PD fabrication. It is not necessary to install the PDs into the APA frames until shortly prior to installation of the APAs into the cryostat.

As noted above, and shown in Figure [fig:5.5-4](#), a total of 10 PDs are installed into each APA frame, with five coming in from each side. The installation will occur with the fully assembled APA frame lying flat on an insertion station table. Prior to installation, the PD cable bundle will be inserted into the APA side tubes. The cable bundle will be pre-assembled prior to installation such that the end of each cable will terminate at the correct slot for the PD to be connected. Our baseline

cable design has also been modified to a single cable with four individual twisted pairs in a single jacket, so each APA side tube will only require 15 cables (three per PD, 30 per APA). These cables extend approximately 30 cm past the end of the APA tubes at the cold electronics end of the APA, and following installation of the APA into the cryostat are connected to long-haul cables for the run to the readout electronics (see Figure [fig:5.8-1](#)).

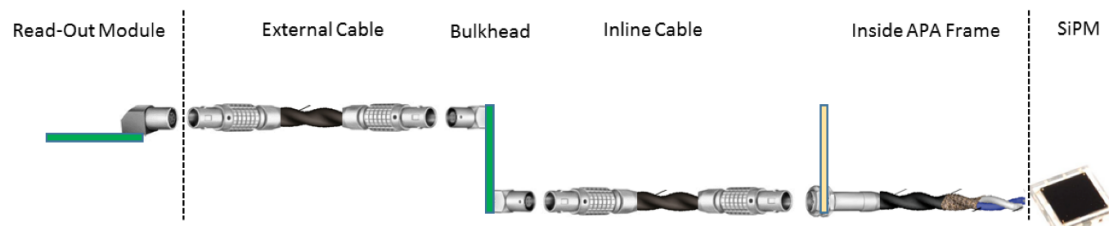


Figure 1.26: Cable assembly for each photon detector readout channel.

[fig:fig:5.8-1](#)

Following this step, five PDs will be inserted into the APA through one side frame, with connections being made between the twisted-pair cables and the SiPM PCB just as the readout end of the detector enters the tube (see Figure [fig:5.8-2](#)). The PD is then inserted the last 10 cm into the frame, and affixed to the inner surface of the APA tube (see Figure [fig:5.8-3](#)). The process is then completed for the five PDs to be inserted from the opposite side.

Following insertion of the PDs, the environmental controls required for the PD WLS materials (UV filtering, temperature and humidity control) will need to be observed for the entire APA.

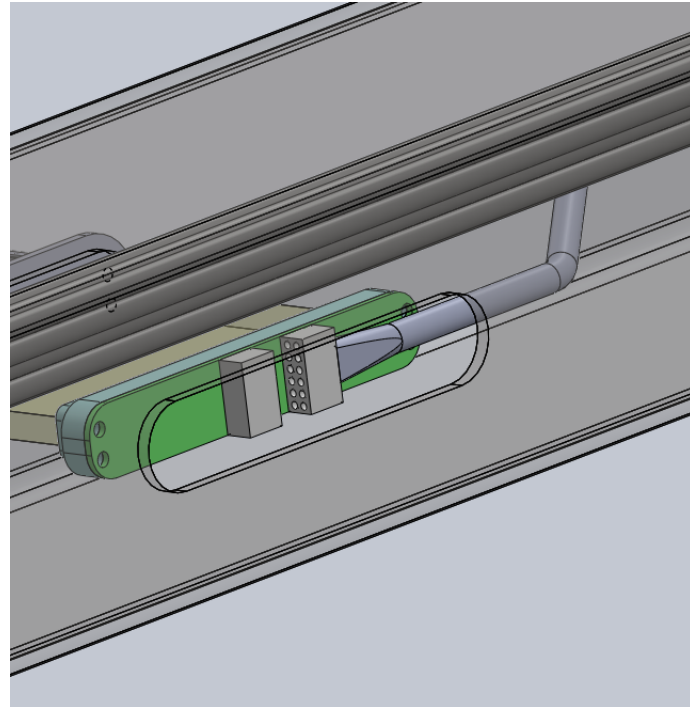


Figure 1.27: Connection between the PD twisted-pair cable and SiPM mounting board.

fig:fig:5.8-2

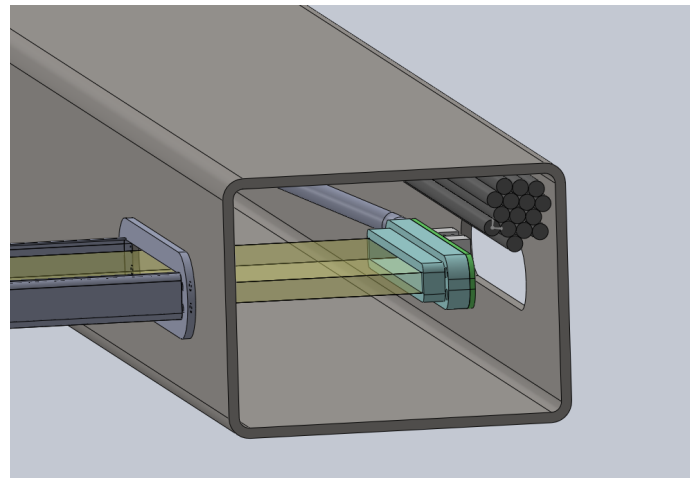


Figure 1.28: Insertion of one PD paddle

fig:fig:5.8-3